Requirements for stress granule recruitment of fused in sarcoma (FUS) and TAR DNA-binding protein of 43 kDa (TDP-43)

Bentmann, Eva ; Neumann, Manuela ; Tahirovic, Sabina ; Rodde, Ramona ; Dormann, Dorothee ; Haass, Christian

Abstract: Cytoplasmic inclusions containing TAR DNA-binding protein of 43 kDa (TDP-43) or Fused in sarcoma (FUS) are a hallmark of amyotrophic lateral sclerosis (ALS) and several subtypes of frontotemporal lobar degeneration (FTLD). FUS-positive inclusions in FTLD and ALS patients are consistently co-labeled with stress granule (SG) marker proteins. Whether TDP-43 inclusions contain SG markers is currently still debated. We determined the requirements for SG recruitment of FUS and TDP-43 and found that cytoplasmic mislocalization is a common prerequisite for SG recruitment of FUS and TDP-43. For FUS, the arginine-glycine-glycine zinc finger domain, which is the protein's main RNA binding domain, is most important for SG recruitment, whereas the glycine-rich domain and RNA recognition motif (RRM) domain have a minor contribution and the glutamine-rich domain is dispensable. For TDP-43, both the RRM1 and the C-terminal glycine-rich domain are required for SG localization. ALS-associated point mutations located in the glycine-rich domain of TDP-43 do not affect SG recruitment. Interestingly, a 25-kDa C-terminal fragment of TDP-43, which is enriched in FTLD/ALS cortical inclusions but not spinal cord inclusions, fails to be recruited into SG. Consistently, inclusions in the cortex of FTLD patients, which are enriched for C-terminal fragments, are not co-labeled with the SG marker poly(A)-binding protein 1 (PABP-1), whereas inclusions in spinal cord, which contain full-length TDP-43, are frequently positive for this marker protein.

DOI: https://doi.org/10.1074/jbc.M111.328757

Neurobiology:

Requirements for stress granule recruitment of fused in Sarcoma (FUS) and TAR DNA binding protein of 43 kDa (TDP-43)

Eva Bentmann, Manuela Neumann, Sabina Tahirovic, Ramona Rodde, Dorothee Dormann and Christian Haass

J. Biol. Chem. published online May 4, 2012

Access the most updated version of this article at doi: 10.1074/jbc.M111.328757

Supplemental material:
http://www.jbc.org/content/suppl/2012/05/04/M111.328757.DC1.html

JBC Papers in Press. Published on May 4, 2012 as Manuscript M111.328757
The latest version is at http://www.jbc.org/cgi/doi/10.1074/jbc.M111.328757

Requirements for Stress Granule Recruitment of Fused in Sarcoma (FUS) and TAR DNA Binding Protein of 43 kDa (TDP-43)*

Eva Bentmann[1], Manuela Neumann[2], Sabina Tahirovic[3], Ramona Rodde[1], Dorothee Dormann[1#], Christian Haass[1,3#]

[1]Adolf-Butenandt-Institute, Biochemistry, Ludwig-Maximilians-University, Schillerstr. 44, 80336 München, Germany
[2]Institute of Neuropathology, University Hospital Zurich, Schmelzbergstr. 12, 8091 Zurich, Switzerland
[3]DZNE - German Center for Neurodegenerative Diseases, Munich, Schillerstr. 44, 80336 München, Germany

***Running title**: *Requirements for stress granule recruitment of FUS and TDP-43*

[#]To whom correspondence should be addressed: Dorothee Dormann or Christian Haass, Adolf-Butenandt-Institute, Biochemistry, Ludwig-Maximilians-University and DZNE-German Center for Neurodegenerative Diseases, Munich, Schillerstr. 44, 80336 Munich, Germany, Tel.: (+49-89) 2180 75471; Fax: (+49-89) 2180 75415; E-mail: dorothee.dormann@dzne.lmu.de or christian.haass@dzne.lmu.de

Keywords: Fused in sarcoma (FUS); TAR DNA binding protein of 43 kDa (TDP-43 or *TARDBP*); Amyotrophic lateral sclerosis (ALS); Frontotemporal lobar degeneration (FTLD); stress granules (SG)

Background: Stress granules (SG) have been implicated in the formation of pathological FUS and TDP-43 inclusions.
Results: SG recruitment of FUS and TDP-43 requires cytosolic mislocalization and their main RNA binding domain and glycine-rich domain.
Conclusion: FUS and TDP-43 have similar requirements for SG recruitment.
Significance: Understanding how FUS and TDP-43 are recruited to SG is critical for understanding FTLD/ALS pathology.

SUMMARY

Cytoplasmic inclusions containing TAR DNA binding protein of 43 kDa (TDP-43) or Fused in sarcoma (FUS) are a hallmark of amyotrophic lateral sclerosis (ALS) and several subtypes of frontotemporal lobar degeneration (FTLD). FUS-positive inclusions in FTLD and ALS patients are consistently co-labeled with stress granule (SG) marker proteins. Whether TDP-43 inclusions contain SG markers is currently still debated. We determined the requirements for SG recruitment of FUS and TDP-43 and found that cytoplasmic mislocalization is a common prerequisite for SG recruitment of FUS and TDP-43. For FUS, the arginine-glycine-glycine zinc finger domain, which is the protein´s main RNA binding domain, is most important for SG recruitment, while the glycine-rich domain and RNA recognition motif (RRM) domain have a minor contribution and the glutamine-rich domain is dispensable. For TDP-43, both the RRM1 and the C-terminal glycine-rich domain are required for SG localization. ALS-associated point mutations located in the glycine-rich domain of TDP-43 do not affect SG recruitment. Interestingly, a 25 kDa C-terminal fragment (CTF) of TDP-43, which is enriched in FTLD/ALS cortical inclusions but not spinal cord inclusions, fails to be recruited into SG. Consistently, inclusions in the cortex of FTLD patients, which are enriched for CTFs, are not co-labeled with the SG marker Poly A binding protein 1 (PABP-1), whereas inclusions in spinal cord, which contain full-length TDP-43, are frequently positive for this marker protein.

Amyotrophic lateral sclerosis (ALS) and frontotemporal lobar degeneration (FTLD) are related neurodegenerative diseases, in which the majority of cases are characterized by the pathological accumulation of the TAR DNA binding protein 43 (TDP-43) or the Fused in

sarcoma (FUS) protein (1). TDP-43 and FUS are DNA/RNA-binding proteins that are involved in transcriptional regulation, pre-mRNA splicing, microRNA processing and mRNA transport (reviewed in (2,3)). Although both proteins exert their function predominantly in the nucleus, pathological TDP-43 and FUS inclusions are mostly observed in the cytoplasm. Strikingly, inclusion-bearing cells often show a loss or reduction of nuclear TDP-43 or FUS staining (4-11). This has led to the hypothesis that loss of nuclear TDP-43 or FUS is a crucial step in disease progression.

Both proteins have multiple RNA binding domains as well as a protein interaction domain predicted to have prion-like properties. TDP-43 has two RNA recognition motif (RRM) domains, RRM1 and RRM2, with RRM1 being the predominant functional RNA binding domain (12). In addition, TDP-43 contains a C-terminal glycine-rich domain, which mediates interactions with other hnRNP proteins and is required for splicing regulation (13). This domain is highly aggregation-prone (14-18) and due to its amino acid composition has been suggested to have prion-like properties (19-22). FUS has multiple RNA binding domains with arginine-glycine-glycine (RGG) motifs, a RRM domain and a zinc finger domain shown to mediate RNA binding (23,24). In addition, FUS contains an N-terminal glutamine-rich domain, which functions as a potent transcriptional activation domain (25) and was predicted to be a prion-like domain (19-21).

The relevance of TDP-43 and FUS in the pathogenesis of ALS and FTLD was strongly supported by the discovery of autosomal dominant mutations within *TARDBP* (the gene encoding TDP-43) and *FUS* in familial forms of ALS (fALS) (6,7,26). So far, almost 40 different *TARDBP* mutations have been reported, most of them are missense mutations in the glycine-rich C-terminal domain. Although it has been claimed that *TARDBP* mutations increase aggregation tendency (14,15,27,28), alter the protein´s cellular localization (29-31) or alter the protein`s half-life and interactions with other proteins (32), the pathogenic mechanism of these mutations is still unclear, since many inconsistencies among different studies have been reported. Pathogenic mutations in the *FUS* gene are mostly clustered in the C-terminal proline-tyrosine nuclear localization signal (PY-NLS) and impair Transportin-mediated nuclear import of FUS (33-36). Interestingly, mutations that show a very severe nuclear import defect, such as P525L, cause an unusually early disease onset and rapid disease progression (37-39), suggesting that impaired nuclear import of FUS is causally linked to the disease (33,40). Even though it is still unclear how reduced nuclear import of FUS leads to neurodegeneration, it has been shown that blockade of Transportin-mediated nuclear import or *FUS* mutations lead to recruitment of FUS into stress granules (SG), implicating SG and reduced nuclear transport in disease pathogenesis (33,34,36,40,41). This is supported by the presence of SG markers in inclusions in ALS/FTLD-FUS patients (33,42).

SG are cytosolic structures that form transiently upon exposure of cells to environmental stress, such as heat, viral infection, oxidative stress or hypoxia (43). They arise from polysomes and store mRNAs encoding housekeeping proteins, but exclude mRNAs encoding chaperones and enzymes involved in damage repair. In addition to mRNAs, SG contain many RNA binding proteins, such as Poly A binding protein 1 (PABP-1) and T cell intracellular antigen 1 (TIA-1), which serve as specific markers for SG (44). In cultured cells, SG formation can be elicited with a variety of stress treatments, such as heat shock (42-44°C), osmotic shock, UV irradiation or substances that elicit mitochondrial and/or oxidative stress (44). SG have also been observed *in vivo* (41,45-47) and SG marker proteins were found to label the pathological FUS inclusions in *post mortem* brains of ALS/FTLD patients (33,42). Thus, it has been suggested that SG might be the precursors of the pathological FUS inclusions in ALS/FTLD-FUS patients (33).

How FUS is recruited to SG is currently unknown. Since FUS is an RNA binding protein, it is conceivable that it is recruited into these structures via its associated mRNAs. Alternatively, protein-protein interactions might be involved in localization of FUS to SG. Interestingly, TIA-1 contains a prion-like glutamine-rich domain that has homology to the N-terminal glutamine-rich domain of FUS and promotes SG assembly by a prion-like aggregation mechanism (48,49). Whether this domain of FUS is required for SG recruitment or aggregation is still unknown.

TDP-43 has also been described to be recruited to SG under various stress conditions (31,50-55) and SG-associated proteins have been identified as TDP-43-interacting proteins (56). However, it is still controversial whether TDP-43 inclusions in human patients contain SG markers. Two studies found a lack of SG markers in TDP-43 inclusions of ALS/FTLD-TDP patients (33,50), while two other studies reported co-labeling of TDP-43 inclusions with SG markers (31,57). Furthermore, it is still not clear if or how *TARDBP* mutations affect SG recruitment. One cell culture study reported that *TARDBP* mutations increase the number of cells with TDP-43 inclusions in response to stress (31), while another group found that mutant (R361S) TDP-43 impairs SG formation (54), and a third study reported that overexpression of mutant (G348C) TDP-43 leads to larger SG (51).

To address how FUS and TDP-43 are recruited into SG, we mapped the domains required for SG recruitment of FUS and TDP-43. In addition, we analyzed the effect of various fALS-associated *TARDBP* mutations on SG recruitment of TDP-43 and further investigated the presence of SG marker proteins in TDP-43 inclusions in ALS/FTLD-TDP cortex and spinal cord.

EXPERIMENTAL PROCEDURES

Cell culture and transfection – Human cervical carcinoma cells (HeLa) were cultured in Dulbecco´s modified Eagle´s medium with Glutamax (Invitrogen) supplemented with 10% (vol/vol) fetal calf serum (Invitrogen) and penicillin/streptomycin (PAA). Transfection of HeLa cells was carried out with Fugene 6 (Roche) or Lipofectamine 2000 (Invitrogen) according to the manufacturer´s instructions. Hippocampal neurons were isolated from embryonic day 18 rats as described previously (58). Neurons were plated at densities of 18 000 cells/cm^2 in 6 cm tissue culture dishes containing poly-L-lysine (1 mg/ml; Sigma-Aldrich)-coated glass coverslips and Neurobasal medium supplemented with 2% B27 and 0.5 mM glutamine (all from Invitrogen). On day *in vitro* (DIV) 7, cultured neurons were transfected with FUS or TDP-43 constructs using Lipofectamine 2000 (Invitrogen) and were analyzed on DIV 9.

Stress and inhibitor treatment – Heat shock was performed by incubating cells for 1 hour in a tissue culture incubator heated to 44°C. For recovery experiments, cells were shifted back to 37°C and incubated another 60 min. Where indicated, cycloheximide (CHX, Sigma) was added at a concentration of 20 µg/ml immediately before shifting cells to 44°C. Clotrimazole (Sigma C6019) was dissolved in DMSO (20 mM stock) and was added to cells under serum-free conditions in OptiMEM (Invitrogen) at a final concentration of 20 µM for 30 min. Sodium (meta)arsenite (Sigma S71287) was dissolved in water (100 mM stock) and was added to cells at a final concentration of 0.5 mM for 30 min.

Antibodies – The following antibodies were used: β-Actin-specific mouse monoclonal antibody clone AC-74 (Sigma); GFP-specific rabbit polyclonal antibody (BD Living Colors); HA-specific mouse monoclonal antibody HA.11 (Covance); horseradish peroxidase (HRP)-coupled rat monoclonal anti-HA antibody 3F10 (Roche); myc-specific mouse monoclonal antibody 9E10 (sc-40, Santa Cruz); PABP-1-specific rabbit polyclonal antibody (Cell Signaling); TDP-43-specific rabbit polyclonal antibody TARDBP (Proteintech); polyclonal antibodies raised against amino acid residues 6-24 of TDP-43 (N-t TDP-43) and amino acid residues 394-414 of TDP-43 (C-t TDP-43) (59); phospho-serine 409/410-specific TDP-43 rat monoclonal antibody clone 1D3 (60); TIA-1-specific goat polyclonal antibody (C-20, Santa Cruz); α-Tubulin-specific mouse monoclonal antibody clone B-5-1-2 (Sigma); βIII-Tubulin-specific rabbit polyclonal antibody clone Tuj1 (Sigma); V5-specific mouse monoclonal antibody (R960-25, Invitrogen). Secondary antibodies for immunoblotting were HRP-coupled goat anti-mouse or anti-rabbit IgGs (Promega). For immunofluorescence stainings, Alexa-488, Alexa-555, Alexa-594 and Alexa-647-conjugated donkey anti-mouse, anti-rabbit, anti-rat or anti-goat IgG (Invitrogen) were used.

cDNA constructs and primers – HA-FUS-WT, HA-FUS-P525L and GFP-Bimax were described in (33). For FUS deletion constructs, the individual domains of FUS were amplified by PCR and PCR products were cloned into the pcDNA3.1/Hygro(-) vector (Invitrogen) via BamHI/XhoI restriction digest. TDP-WT-V5, myc-TDP-WT and TDP-Δ1-173-V5 were described in (61). For TDP-NLSmut, amino acids 82-84 of TDP-WT-V5 were mutated to alanine by QuikChange mutagenesis (Stratagene) as described

by (62). ALS-associated point mutations (A315T, M337V and G348C) were introduced into myc-TDP-WT or TDP-NLSmut-V5 by QuikChange mutagenesis (Stratagene). NLSmut-ΔC encoding amino acids 1-273 of human TDP-43 was amplified by PCR and after BamHI/XbaI restriction digest was cloned into the pcDNA6/V5-His vector (Invitrogen), which contained a stop codon between the V5 and the polyhistidine tag sequence. GFP-tagged constructs were generated by subcloning the respective sequences into pEGFP-C1 (Clontech). For all constructs, sequence integrity was verified by sequencing. Oligonucleotides sequences are available upon request.

Human post mortem tissue – Histological analysis included five cases of FTLD-TDP (FTLD-TDP subtype A (n=2), subtype B (n=2) and subtype C (n=1) according to (63)) and four ALS cases with TDP-43 pathology.

Immunocytochemistry and immunohisto-chemistry – For immunocytochemistry of Hela cells, cells were fixed for 15 min in 4% paraformaldehyde in PBS, permeabilized for 5 min in 0.2% Triton X-100 with 50 mM NH_4Cl and subsequently blocked for 20-30 min in 5% donkey serum in PBSS (PBS with 0.1% saponin). Cells were stained with the indicated primary and secondary antibodies diluted in 5% donkey serum in PBSS for 30 min and were washed three to five times in PBSS. To visualize nuclei, cells were stained with TO-PRO-3 iodide (Invitrogen, 1:500 in PBS) for 15 min and were washed three times in PBS. Coverslips were mounted onto glass slides using ProLong Gold Antifade Reagent (Invitrogen).

For immunocytochemistry of hippocampal neurons, neurons were fixed with 4% paraformaldehyde on DIV 9, quenched in 50 mM ammonium chloride for 10 min and permeabilized with 0.1% Triton X-100 for 3 min. After blocking with 2% fetal bovine serum (Invitrogen), 2% bovine serum albumin (Sigma-Aldrich), and 0.2% fish gelatin (Sigma-Aldrich) dissolved in PBS, neurons were incubated with respective primary and secondary antibodies diluted in 10% blocking solution. 4'-6-diamidino-2-phenyl-indol (DAPI, Invitrogen) was used as a nuclear counterstain.

Immunohistochemistry on human *post mortem* material was performed on 5 µm thick sections of formalin-fixed, paraffin-embedded sections from spinal cord or hippocampus with the N- and C-terminal TDP-43-specific antibodies and anti-PABP-1 using the NovoLink™ Polymer Detection Kit (Novocastra) and developed with 3,3'-diaminobenzidine. Microwave antigen retrieval was performed for all stainings. Double-label immunofluorescence for PABP-1 and pTDP-43 was performed using Alexa-488 and -594 conjugated secondary antibodies. DAPI (Vector Laboratories) was used for nuclear counterstaining.

Image acquisition and quantification – Confocal images were obtained with an inverted laser scanning confocal microscope (Zeiss Axiovert 200M) with a 63x/1.4 N.A. oil immersion lens, using a pinhole diameter of 1 Airy unit in the red channel. Pictures were taken and analyzed with the LSM 510 confocal software (Zeiss). For HeLa cells, single confocal images were taken in the plane of the largest cytosolic area. For neurons, a series of images along the z axis was taken and projected into a single image using the maximal projection tool of the LSM 510 software. Immunofluorescence images of brain sections were obtained by wide-field fluorescence microscopy (BX61 Olympus with digital camera F-view, Olympus).

Nuclear and cytosolic localization was quantified with the LSM 510 colocalization tool as described in (33). Stress granule localization was quantified with Image J as follows: Image identity was blinded and FUS or TDP-43 (green)/TIA-1 (red) double positive cytoplasmic granules as well as the entire cell were manually encircled to measure fluorescence intensities of the green channel. After background subtraction, the percentage of FUS or TDP-43 in SG was calculated. For each condition, 10-20 cells were analyzed. Means across all cells and standard deviations were calculated.

Cell lysates and immunoblotting – Total cell lysates were prepared in ice cold radioimmunoprecipitation assay (RIPA) buffer freshly supplemented with complete EDTA-free protease inhibitor cocktail (Roche) for 15 min on ice. Lysates were sonicated in a bioruptor (Diagenode, 45 seconds on high) and protein concentration was determined by BCA protein assay (Pierce). Equal amounts of protein were separated by SDS-PAGE, transferred onto a PVDF membrane (Immobilon-P, Millipore) and analyzed by immunoblotting using the indicated antibodies. Bound antibodies were detected with the

chemiluminescence detection reagents ECL (Amersham) or Immobilon (Millipore).

RNA binding assay – RNA binding of FUS and TDP-43 domains was determined in an *in vitro* RNA binding assay according to (24). Briefly, proteins were *in vitro* transcribed and translated using the TNT T7 Coupled Reticulocyte Lysate System (Promega) and were labeled with 20 µCi [^{35}S] methionine (Amersham Biosciences). Strep-Tactin sepharose (IBA) was blocked with 200 µg/ml yeast tRNA (Roche) and 0.125 mg/ml bovine serum albumin (BSA, NEB) in wash buffer (10 mM Tris-HCl pH 7.4, 100 mM NaCl, 2.5 mM $MgCl_2$, 0.5 mM DTT, 0.5 mM EGTA, 0.5 % Triton X-100, 10% glycerol) for 30 min at 4°C. Afterwards, biotinylated RNA oligonucleotides (UG_{12}: UGUGUGUGUGUGUGUGUGUGUG; GGUG: UUGUAUUUUGAGCUAGUUUGGUGAU or CCUC: UUGUAUUUUGAGCUAGUUUCCUCAU, all from Thermo Fisher Scientific) were bound to the preblocked sepharose beads. Beads were rinsed twice with wash buffer and were incubated with radiolabeled samples for 10 min at 4°C in blocking buffer. Beads were washed five times in wash buffer and boiled 5 min in Lämmli buffer. Bound radiolabeled proteins were separated by SDS-PAGE and visualized by fluorography. 10% of the radiolabeled sample was directly used for SDS-PAGE and fluorography to visualize the input of radiolabeled protein.

RESULTS

The RGG-zinc finger domain of FUS is most important for SG recruitment, while the glutamine-rich domain is dispensable – We and others previously found that cytosolically mislocalized FUS is recruited to SG upon cellular stress (33,34,41). It is however still unknown whether cytosolic FUS is recruited into SG via its bound mRNAs or via protein-protein interactions, involving for example its TIA-1-related N-terminal domain, or even both. To determine which domains are responsible for recruitment of FUS to SG, we expressed individual FUS domains in HeLa cells with an N-terminal HA-tag and analyzed their SG recruitment in comparison to full-length FUS (see Fig. 1A for a schematic diagram). To this end, we introduced the P525L mutation into the PY-NLS of the respective constructs, since this mutation causes cytosolic retention of FUS and allows its efficient recruitment to TIA-1-positive SG (33). In contrast, constructs carrying a wild-type (WT) PY-NLS were almost exclusively nuclear and hence were not recruited to SG upon cellular stress (Fig. S1).

Initially, we investigated a variety of stress conditions, such as heat shock (44°C), oxidative stress caused by sodium arsenite treatment and mitochondrial stress caused by clotrimazole treatment, for their ability to induce SG formation. Consistent with our previous findings (33), FUS-WT was located in the nucleus and therefore was not recruited to SG upon cellular stress (Fig. 1B, upper panels). In contrast, FUS-P525L was efficiently recruited into SG under all stress conditions examined (Fig. 1B, lower panels). FUS-P525L-positive granules were bona fide stress granules, since they were co-localized with the SG marker TIA-1 and disassembled upon cycloheximide treatment or recovery from heat stress (Fig. S2A). SG recruitment of FUS-P525L was not a cell type specific phenomenon, since it could also be observed in primary hippocampal neurons (Fig. 1C) and in SH-SY5Y neuroblastoma cells (Fig. S2B).

Using heat shock as stress condition, we next examined how well the individual domains of FUS are recruited to SG (see schematic diagram in Fig. 2A). To obtain quantitative information, we measured the percentage of FUS protein localized in TIA-1 positive SG (see "experimental procedures" for details). In contrast to full-length FUS-P525L, the glutamine-rich domain (Q) remained diffusely distributed in the cytosol after heat shock and no granular localization became evident, even though TIA-1-positive SG formed in transfected cells (Fig. 2B and C). Thus, despite its homology to the prion-like domain of TIA-1 (48,49), the Q domain of FUS does not seem to be involved in SG recruitment. The glycine-rich domain (G) and the RRM domain (R) remained predominantly diffusely cytosolic, but small amounts were found in TIA-1-positive SG (Fig. 2B and C). Finally, the C-terminal RGG-zinc finger domain (Z), which was rendered cytosolic by addition of the P525L mutation (Z_{P525L}), showed more SG recruitment than all other domains examined. Since the HA-tagged Q and Z_{P525L} domain showed very weak expression compared to the other constructs and could not be detected by Western blot (Fig. S3), we expressed these apparently unstable domains as GFP fusion proteins

along with GFP-FUS_{P525L} as a control. This yielded higher expression levels (Fig. S4A) and confirmed that the Z_{P525L} domain shows SG association, whereas the Q domain does not (Fig. S4B).

Since our quantitative analysis revealed that none of the individual domains was recruited to SG to the same extent as the full-length protein (Fig. 2C), we analyzed combinations of the three domains (RZ_{P525L}, GRZ_{P525L} and GR) and asked if this would enhance SG recruitment. Indeed, the combination of these domains showed an additive effect compared to the individual domains (Fig. 2B and C), suggesting that all three domains contribute to SG recruitment. Finally, we analyzed combinations of the Q domain with other domains (QGR, QG), to exclude that the Q domain might have a different effect in the context of the other domains. However, QGR and QG did not differ in their SG localization from GR and G, respectively, demonstrating that the Q domain is indeed dispensable for SG recruitment. Consistently, the GRZ_{P525L} protein, which lacks the Q domain, was recruited to SG equally well as full-length FUS-P525L. Furthermore, the relatively weak SG recruitment efficiency of the QGR protein confirms that the C-terminal Z domain plays the most important role for SG association of FUS.

In summary, the RGG-zinc finger domain (Z) is the most important domain for SG recruitment of FUS. The glycine-rich domain (G) and to a minor extent the RRM domain (R) also contribute to SG recruitment, whereas the prion-like glutamine-rich domain (Q) is dispensable.

The RGG-zinc finger domain is the main RNA binding domain of FUS – To explore if SG recruitment of the different FUS domains can be correlated with their ability to bind RNA, we examined their RNA binding capacity in an RNA binding assay. To this end, we *in vitro* translated the same FUS constructs and performed a pull down assay with biotinylated RNA oligonucleotides immobilized on streptavidin beads. Since FUS is known to preferentially bind to UG-rich sequences, specifically to oligonucleotides containing a GGUG motif (24), we first tested the ability of FUS-WT to bind to UG_{12} or a GGUG-containing oligonucleotide (UUGUAUUUUGAGCUAGUUUGGUGAU, named GGUG). The same oligonucleotide with a CCUC motif (named CCUC) was used as a negative control. Consistent with the previously reported finding that FUS binds to UG-rich sequences, FUS-WT was efficiently pulled down by UG_{12} and to a lesser extent by GGUG, but not CCUC (Fig. 3A).

Using UG_{12} as RNA bait, we next examined the RNA binding capacity of the individual FUS domains and combinations thereof (Fig. 3B). This demonstrated that only proteins containing the Z domain (Z_{P525L}, RZ_{P525L} and GRZ_{P525L}) showed efficient and selective binding to UG_{12} RNA. (Note that compared to Z_{P525L}, RZ_{P525L} and GRZ_{P525L} showed stronger signals already in the input gel and therefore signals obtained in the pulldown cannot be compared directly.) In contrast, the Q, G and R domain and different combinations thereof (GR, QGR, QG) were not pulled down in our RNA binding assay, demonstrating that Q, G and R show no or only weak binding to UG_{12} RNA. Thus, the C-terminal Z domain seems to be responsible for the preferential binding to UG-rich RNA. Interestingly, the domain with the highest RNA binding capacity (Z) was the one most important for SG recruitment (Fig. 2). This correlation suggests that FUS might be recruited to SG by virtue of its RNA binding capacity. The domains that contribute to SG recruitment to a lesser extent (G and R) showed no RNA binding capacity in our *in vitro* binding assay, suggesting that they might contribute to SG recruitment through other means, possibly protein-protein interactions.

Cytosolic mislocalization is a prerequisite for SG recruitment of TDP-43 – Similar to FUS, TDP-43 has been described to be localized in SG under various experimental conditions (31,50-55). Since cytosolic mislocalization is a prerequisite for efficient SG recruitment of FUS (Fig. 1 and (33,41)), we speculated that this might also be the case for TDP-43. To test this hypothesis, we mutated three essential amino acids of the classical bipartite nuclear localization signal (62) and analyzed SG recruitment of this artificial NLS mutant (NLSmut, see Fig. 4A for a schematic diagram) in comparison to wild-type TDP-43 (TDP-WT) upon exposure to different stressors. TDP-WT was predominantly nuclear with and without stress and was not detectable in cytoplasmic granules (Fig. 4B, upper panels). In contrast, the partially cytosolic NLSmut protein was readily detectable in TIA-1-positive SG upon heat shock, clotrimazole treatment and sodium arsenite treatment (Fig. 4B, lower panels). TDP-43-positive granules dissolved upon cycloheximide

treatment or recovery from heat stress (Fig. S5A), demonstrating that they are indeed SG and not protein aggregates. Moreover, SG recruitment of NLSmut but not TDP-WT was observed in primary hippocampal neurons (Fig. 4C) and SH-SY5Y cells (Fig. S5B). Thus, in all cell types examined, only cytosolic but not nuclear TDP-43 is efficiently recruited to SG.

To corroborate this finding, we expressed an Importin α/β inhibitor peptide fused to GFP (GFP-Bimax) (64) in HeLa cells. Consistent with our previous findings (33), this caused endogenous TDP-43 to accumulate in the cytosol (Fig. 5). In line with the view that cytosolic mislocalization of TDP-43 is required for SG recruitment, endogenous TDP-43 was detectable in heat shock-induced SG only when its nuclear import was blocked by expression of the GFP-Bimax inhibitor (Fig. 5). In contrast, in control (GFP) transfected cells, TDP-43 remained nuclear and was not detectable in SG upon heat shock. Together these findings demonstrate that similar to FUS, SG recruitment of TDP-43 requires at least a partial mislocalization of the nuclear protein to the cytosol.

ALS-associated TARDBP mutations do not affect nuclear localization or SG recruitment - Despite extensive research over the last few years, the pathogenic mechanism of ALS-associated *TARDBP* mutations remains unclear. Some *TARDBP* mutations have been reported to cause cytosolic missorting of the protein (30,31), however this could not be confirmed in other studies (28,32,51). Furthermore, it is still not clear if and how *TARDBP* mutations affect SG recruitment, since controversial findings have been reported (31,51,54).

Since our data above imply that SG recruitment could be indicative of cytosolic mislocalization, we examined the localization of three well-studied ALS-associated *TARDBP* mutations (A315T, M337V and G348C) upon heat shock, to see if these mutants would be preferentially detected in SG. However, none of the three examined ALS-associated point mutants showed detectable localization in TIA-1-positive SG upon heat shock (44°C), instead they were located entirely in the nucleus like TDP-WT (Fig. 6A, for expression levels see Fig. 6B). Consistently, a quantification of the amount of nuclear/cytosolic TDP-43 in cells cultured under normal culture conditions (37°C) demonstrated that the three point mutants had an almost exclusive nuclear localization and did not differ from the WT protein (Fig. 6C). Thus, the examined ALS-associated *TARDBP* mutations (A315T, M337V and G348C) do not cause cytoplasmic mislocalization or SG recruitment of TDP-43.

Since it is possible that *TARDBP* mutations may affect SG recruitment once the protein has accumulated in the cytosol, for example as a consequence of axonal injury (65) or reduced expression of nuclear import factors (66), we introduced the same ALS-associated *TARDBP* mutations into the NLS mutant of TDP-43, to see if the mutations would impair or enhance SG recruitment of cytosolic TDP-43. As expected, TDP-NLSmut$_{A315T}$, NLSmut$_{M337V}$ and NLSmut$_{G348C}$ showed the same cytosolic mislocalization as NLSmut (Fig. 7A, left panels) and similar expression levels (Fig. 7B). Upon cellular stress elicited by clotrimazole treatment, all mutants were readily detectable in TIA-1-positive SG (Fig. 7A, right panels). A quantitative analysis of SG recruitment showed that the ALS-associated *TARDBP* mutants were incorporated into SG to a similar degree as NLSmut (Fig. 7C).

Taken together, the examined ALS-associated point mutations in the glycine-rich C-terminal domain of TDP-43 (A315T, M337V and G348C) neither cause cytosolic mislocalization of nuclear TDP-43, nor do they affect SG recruitment of cytosolic TDP-43.

TDP-43 inclusions in spinal cord but not in cortex contain the SG marker PABP-1 – Even though TDP-43 can be recruited to SG under various experimental conditions (this study and (31,50,51,53,56)), it is still controversial whether TDP-43 inclusions in ALS/FTLD patients contain SG marker proteins. Two studies showed a lack of SG markers in TDP-43 inclusions (33,50), while two other studies reported co-labeling of TDP-43 inclusions with SG markers (31,57). We reasoned that these discrepancies might be due to the fact that TDP-43 inclusions differ in their TDP-43 species composition, with inclusions in the spinal cord of ALS and FTLD patients containing predominantly full-length TDP-43 and inclusions in the cortex and hippocampus of ALS and FTLD patients being highly enriched for C-terminal fragments (CTFs) of approximately 25 kDa (59,60).

To see if differences in the TDP-43 species composition might account for the different results

regarding co-labeling of TDP-43 inclusions with SG markers, we stained sections of spinal cord or cortex (hippocampus) from ALS-TDP and FTLD-TDP cases with N- and C-terminal TDP-43 antibodies as well as antibodies specific for the SG marker protein PABP-1. Inclusions in the spinal cord were consistently labeled with both N- and C-terminal TDP-43 antibodies, while inclusions in the cortex, including those in dentate granule neurons, were only labeled with the C-terminal antibody (Fig. 8), confirming previous results (59). Cortical TDP-43 inclusions were not immunoreactive for PABP-1, confirming our previous results (33). However, we revealed PABP-1 positivity in a subset (~66%) of TDP-43-positive inclusions in the spinal cord, as demonstrated by double-label immunofluorescence (Fig. 8 and Fig. S6). Thus, TDP-43 inclusions in spinal cord and cortex show a differential co-labeling for the SG marker protein PABP-1.

25 kDa C-terminal fragment (CTF) of TDP-43 is not recruited to SG – We speculated that the differences in SG marker co-labeling of TDP-43 inclusions in different tissues may be due to the presence of different TDP-43 species, with distinct abilities to be recruited to SG. Since inclusions in cortex are highly enriched in CTFs of TDP-43 (59,60) and are negative for PABP-1 (Fig. 8), we wondered if CTFs may be unable to associate with SG. To test this hypothesis, we expressed a CTF of approximately 25 kDa (TDPΔ1-173, see Fig. 9A for a schematic diagram) in HeLa cells and analyzed its recruitment to TIA-1-positive SG upon cellular stress. Like NLSmut, TDPΔ1-173 was partially localized in the cytosol under control conditions (Fig. 9B, left panels), since it lacks the N-terminal domain including the protein´s NLS (Fig. 9A). However, in contrast to NLSmut, TDPΔ1-173 remained diffusely distributed in the cytosol upon clotrimazole treatment and consistent with our hypothesis was very poorly incorporated into TIA-1-positive SG (Fig. 9B, right panels and C). Since TDPΔ1-173 showed very low expression levels compared to NLSmut (Fig. 9D), we repeated the experiment with GFP-tagged TDPΔ1-173, to exclude that the lack of SG association was simply due to low protein levels. Similar to V5-tagged TDPΔ1-173, the highly expressed GFP-tagged TDPΔ1-173 remained diffusely distributed upon cellular stress (Fig. S7A and B). Thus, independent of expression levels, the 25 kDa CTF fails to associate with SG. This might explain why cortical TDP-43 inclusions, which are highly enriched in CTFs and contain little full-length TDP-43 (Fig. 8 and (59,60)), are not co-labeled with SG marker proteins.

The C-terminal glycine-rich domain of TDP-43 is required for efficient SG recruitment – Surprisingly, not only deletion of amino acids 1-173, but also deletion of the C-terminal glycine-rich domain from TDP-43 NLSmut (NLSmut-ΔC, see schematic diagram in Fig. 9A) led to a strong reduction in SG recruitment, since NLSmut-ΔC remained mostly diffusely distributed in the cytoplasm upon cellular stress (Fig. 9B and C). Expression level differences could not account for this effect, since NLSmut-ΔC was at least as well expressed as NLSmut (Fig. 9D). To test whether reduced RNA binding may be responsible for reduced SG recruitment of NLSmut-ΔC, we performed an RNA binding assay using UG_{12} RNA as a TDP-43-specific target sequence (12). As expected, TDP-WT was efficiently pulled down by UG_{12} (Fig. 10A). Interestingly, TDP-WT bound equally well to GGUG but not the corresponding CCUC oligonucleotide, consistent with the recent finding that TDP-43 can bind to sequences other than UG repeats (67).

Using UG_{12} as RNA bait, we next compared the RNA binding capacity of full-length TDP-43 (WT and NLSmut) and the two deletion mutants NLSmutΔC and Δ1-173. The full length proteins were specifically pulled down in our RNA binding assay, while TDP-Δ1-173, which lacks the protein´s main RNA recognition motif (RRM1) (12), failed to bind to UG_{12} RNA (Fig. 10B), which might explain why this fragment is not recruited to SG in FTLD/ALS patients (Fig. 8) and in cultured cells (Fig. 9). In contrast, NLSmut-ΔC bound to UG_{12} RNA as efficiently as full-length TDP-43 (Fig. 10B), demonstrating that the reduced SG recruitment capacity of this deletion mutant cannot be explained by reduced RNA binding. Thus, the glycine-rich domain seems to possess other, so far unknown features that are important for SG recruitment.

In summary, RNA binding of TDP-43 depends on the N-terminal RRM1 domain, but not the C-terminal glycine-rich domain. Since both domains are required for SG recruitment of TDP-43, we suggest that RNA binding plus additional features encoded in the C-terminal glycine-rich

domain, such as protein-protein interactions, might contribute to SG recruitment of TDP-43.

DISCUSSION

Two different mechanisms how FUS and TDP-43 are recruited to SG can be envisaged: First, since both proteins have multiple RNA binding motifs (12,24,68), it is conceivable that they are recruited into SG via bound mRNAs. Second, protein-protein interactions with other SG-associated proteins could be involved. Our results suggest that RNA binding plays a crucial role for SG recruitment of both FUS and TDP-43, since deletion mutants lacking the principal RNA binding domains (Z domain of FUS and RRM1 domain of TDP-43) showed poor recruitment to SG. This correlation between RNA binding and SG recruitment suggests that FUS and TDP-43 might be recruited into SG through binding to UG-rich RNA sequences (see model in Fig. 11), although we cannot exclude that protein-protein interactions mediated by the Z and RRM1 domain are involved as well.

In addition, domains that did not bind to UG-rich RNA in our *in vitro* assay (G and R domain of FUS and the C-terminal glycine-rich domain of TDP-43) seem to contribute to SG recruitment as well, since deletion of these domains impaired SG recruitment. Given their lack of RNA binding, these domains may contribute to SG recruitment by providing protein-protein interactions with other SG proteins (symbolized by protein X and Y in Fig. 11). However, we cannot exclude that these putative protein-interacting domains bind to RNA sequences not represented in our *in vitro* binding assay and that these protein-RNA interactions contribute to SG recruitment. Indeed, recent cross-linking and immunoprecipitation (CLIP) experiments have shown that FUS can bind to AU-rich stem loop structures (69) and TDP-43 can bind to sequences other than UG repeats (67). Which domain(s) of FUS and TDP-43 mediate binding to these alternative target sequences remains to be investigated.

Our finding that the C-terminal glycine-rich domain of TDP-43 (amino acid residues 274-414) is required for efficient SG recruitment is consistent with previously published data showing that residues 268-315 are necessary for localization of TDP-43 within SG (50,51). Since the C-terminal domain has been reported to mediate protein-protein interactions, such as interactions with other heterogenous ribonucleoproteins (hnRNPs) (13), including FUS (70), it seems likely that protein-protein interactions contribute to SG recruitment of TDP-43, although the protein(s) involved remain to be identified (protein X in Fig. 11). Freibaum and colleagues identified numerous proteins involved in translation and SG-associated proteins as TDP-43-interacting proteins (56). Furthermore, TDP-43 and TIA-1 were found to interact in co-immunoprecipitation assays, however, this was only seen upon overexpression of both proteins (31). Nevertheless, TIA-1 and other SG-associated proteins are obvious candidates for proteins that recruit TDP-43 into SG via its C-terminal domain.

Although we did not observe myc- or V5-tagged TDP-WT or endogenous TDP-43 in SG after various stress treatment (Fig. 4-7), it is possible that very small amounts of TDP-43, undetectable by our antibodies, are present in SG under these conditions. That this might be the case is suggested by several reports describing at least small amounts of wild-type TDP-43 in SG upon various stress treatments (31,50,51,53,54,56). Nevertheless, we could show that an artificial mutation in the TDP-43 NLS (NLSmut) or inhibition of Importin α/β-mediated nuclear import readily caused SG localization of TDP-43 upon cellular stress. We therefore suggest that cytosolic mislocalization is a prerequisite for recruitment of TDP-43 into SG. Cytosolic mislocalization may be artificially caused by high expression levels of TDP-WT and thus may allow unphysiological SG recruitment. Under physiological expression levels we suggest that a nuclear import defect as the primary hit and cellular stress as the second hit are required for SG recruitment of TDP-43 (33,40). *In vivo*, axonal injury (65) or reduced expression of nuclear transport factors, such as Cellular Apoptosis Susceptibility protein (CAS) and Importin-α2 (66), might constitute such a primary hit leading to the cytoplasmic mislocalization of TDP-43 in ALS/FTLD-TDP patients.

What remains enigmatic is the cellular mechanism of ALS-associated *TARDBP* mutations. In contrast to ALS-associated *FUS* mutations, *TARDBP* mutations in the glycine-rich C-terminal domain (A315T, M337V and G348C) did not affect nuclear localization in our study, consistent with previous reports (28,32,51). Whether ALS-associated *TARDBP* mutations affect SG formation

was controversial. Two studies reported that *TARDBP* mutations increase the number or size of SG, suggesting a toxic gain-of-function mechanism (31,51), while another group found that R361S is a loss-of-function mutation with regard to SG formation, leading to fewer SG (54). In our study, the percentage of TDP-NLSmut in SG was not significantly altered by the presence of ALS-associated point mutations (A315T, M337V and G348C), despite the importance of the C-terminal domain for SG recruitment. However, it remains possible that the dynamics of SG formation or dissolution are affected by ALS-associated *TARDBP* mutations, as recently suggested for R361S (54).

Another dispute that has remained unresolved is whether TDP-43 inclusions in FTLD and ALS patients contain SG marker proteins or not. Two studies reported a co-labeling of TDP-43 inclusions with SG markers (31,57), while two other studies did not find evidence for SG marker co-labeling (33,50). Our data suggest that SG marker co-labeling is dependent on the presence of full-length TDP-43, which is much more abundant in spinal cord inclusions than in cortical TDP-43 inclusions (this study and (59,60)). We therefore suggest that the reported discrepancies could be due to the presence of different TDP-43 species in inclusions in different regions of the central nervous system. How CTFs are generated and why cortical TDP-43 inclusions are highly enriched in these fragments is still unclear. The absence of SG markers from CTF-containing inclusions suggests that these inclusions either arise independently of SG or that CTFs dissociate from SG upon proteolytic cleavage of full-length TDP-43, presumably due to its reduced RNA binding capacity. How exactly SG relate to CTF generation and TDP-43 inclusion formation remains to be investigated.

The presence of SG marker proteins and RNA in pathological FUS or TDP-43 inclusions has led to the hypothesis that these inclusions could arise from stress granules (31,33,42,55). Indeed, various forms of stress have been implicated in the pathogenesis of ALS, including oxidative stress, mitochondrial dysfunction, damage to the vasculature and inflammatory reactions (71-73). Even though it remains to be seen whether SG are actually pathogenic or protective, this model offers a plausible mechanism for how pathological aggregation of cytosolic FUS or TDP-43 might be triggered in response to cellular stress. Recruitment into SG most likely increases the local FUS or TDP-43 concentration, which might seed aggregation of these otherwise soluble proteins in a prion-like manner (74). Whether the prion-like domains of FUS and TDP-43 are secondarily involved in seeding aggregation remains to be seen. We would like to note that so far cellular models were unable to recapitulate bona fide FUS or TDP-43 aggregation, since FUS or TDP-43-containing SG are rapidly disassembled upon stress removal ((41) and this study). We therefore believe that additional hits or chronic stress might be needed for irreversible aggregation of SG localized proteins (40).

REFERENCES

1. Mackenzie, I. R., Rademakers, R., and Neumann, M. (2010) *Lancet Neurol* **9**, 995-1007
2. Buratti, E., and Baralle, F. E. (2008) *Front Biosci* **13**, 867-878
3. Lagier-Tourenne, C., and Cleveland, D. W. (2009) *Cell* **136**, 1001-1004
4. Neumann, M., Sampathu, D. M., Kwong, L. K., Truax, A. C., Micsenyi, M. C., Chou, T. T., Bruce, J., Schuck, T., Grossman, M., Clark, C. M., McCluskey, L. F., Miller, B. L., Masliah, E., Mackenzie, I. R., Feldman, H., Feiden, W., Kretzschmar, H. A., Trojanowski, J. Q., and Lee, V. M. (2006) *Science* **314**, 130-133
5. Arai, T., Hasegawa, M., Akiyama, H., Ikeda, K., Nonaka, T., Mori, H., Mann, D., Tsuchiya, K., Yoshida, M., Hashizume, Y., and Oda, T. (2006) *Biochem Biophys Res Commun* **351**, 602-611
6. Kwiatkowski, T. J., Jr., Bosco, D. A., Leclerc, A. L., Tamrazian, E., Vanderburg, C. R., Russ, C., Davis, A., Gilchrist, J., Kasarskis, E. J., Munsat, T., Valdmanis, P., Rouleau, G. A., Hosler, B. A., Cortelli, P., de Jong, P. J., Yoshinaga, Y., Haines, J. L., Pericak-Vance, M. A., Yan, J., Ticozzi, N., Siddique, T., McKenna-Yasek, D., Sapp, P. C., Horvitz, H. R., Landers, J. E., and Brown, R. H., Jr. (2009) *Science* **323**, 1205-1208

7. Vance, C., Rogelj, B., Hortobagyi, T., De Vos, K. J., Nishimura, A. L., Sreedharan, J., Hu, X., Smith, B., Ruddy, D., Wright, P., Ganesalingam, J., Williams, K. L., Tripathi, V., Al-Saraj, S., Al-Chalabi, A., Leigh, P. N., Blair, I. P., Nicholson, G., de Belleroche, J., Gallo, J. M., Miller, C. C., and Shaw, C. E. (2009) *Science* **323**, 1208-1211
8. Neumann, M., Rademakers, R., Roeber, S., Baker, M., Kretzschmar, H. A., and Mackenzie, I. R. (2009) *Brain* **132**, 2922-2931
9. Lashley, T., Rohrer, J. D., Bandopadhyay, R., Fry, C., Ahmed, Z., Isaacs, A. M., Brelstaff, J. H., Borroni, B., Warren, J. D., Troakes, C., King, A., Al-Saraj, S., Newcombe, J., Quinn, N., Ostergaard, K., Schroder, H. D., Bojsen-Moller, M., Braendgaard, H., Fox, N. C., Rossor, M. N., Lees, A. J., Holton, J. L., and Revesz, T. (2011) *Brain* **134**, 2548-2564
10. Mackenzie, I. R., Ansorge, O., Strong, M., Bilbao, J., Zinman, L., Ang, L. C., Baker, M., Stewart, H., Eisen, A., Rademakers, R., and Neumann, M. (2011) *Acta Neuropathologica* **122**, 87-98
11. Mackenzie, I. R., Munoz, D. G., Kusaka, H., Yokota, O., Ishihara, K., Roeber, S., Kretzschmar, H. A., Cairns, N. J., and Neumann, M. (2011) *Acta Neuropathologica* **121**, 207-218
12. Buratti, E., and Baralle, F. E. (2001) *The Journal of biological chemistry* **276**, 36337-36343
13. Buratti, E., Brindisi, A., Giombi, M., Tisminetzky, S., Ayala, Y. M., and Baralle, F. E. (2005) *The Journal of Biological Chemistry* **280**, 37572-37584
14. Johnson, B. S., Snead, D., Lee, J. J., McCaffery, J. M., Shorter, J., and Gitler, A. D. (2009) *The Journal of Biological Chemistry* **284**, 20329-20339
15. Nonaka, T., Kametani, F., Arai, T., Akiyama, H., and Hasegawa, M. (2009) *Hum Mol Genet* **18**, 3353-3364
16. Furukawa, Y., Kaneko, K., and Nukina, N. (2011) *Biochimica et biophysica acta* **1812**, 1577-1583
17. Zhang, Y. J., Xu, Y. F., Cook, C., Gendron, T. F., Roettges, P., Link, C. D., Lin, W. L., Tong, J., Castanedes-Casey, M., Ash, P., Gass, J., Rangachari, V., Buratti, E., Baralle, F., Golde, T. E., Dickson, D. W., and Petrucelli, L. (2009) *Proc Natl Acad Sci U S A* **106**, 7607-7612
18. Yang, C., Tan, W., Whittle, C., Qiu, L., Cao, L., Akbarian, S., and Xu, Z. (2010) *PLoS One* **5**, e15878
19. Gitler, A. D., and Shorter, J. (2011) *Prion* **5**, 179 - 187
20. Udan, M., and Baloh, R. H. (2011) *Prion* **5**, 1-5
21. Cushman, M., Johnson, B. S., King, O. D., Gitler, A. D., and Shorter, J. (2010) *Journal of Cell Science* **123**, 1191-1201
22. Fuentealba, R. A., Udan, M., Bell, S., Wegorzewska, I., Shao, J., Diamond, M. I., Weihl, C. C., and Baloh, R. H. (2010) *The Journal of Biological Chemistry* **285**, 26304-26314
23. Iko, Y., Kodama, T. S., Kasai, N., Oyama, T., Morita, E. H., Muto, T., Okumura, M., Fujii, R., Takumi, T., Tate, S., and Morikawa, K. (2004) *The Journal of Biological Chemistry* **279**, 44834-44840
24. Lerga, A., Hallier, M., Delva, L., Orvain, C., Gallais, I., Marie, J., and Moreau-Gachelin, F. (2001) *The Journal of Biological Chemistry* **276**, 6807-6816
25. Prasad, D. D., Ouchida, M., Lee, L., Rao, V. N., and Reddy, E. S. (1994) *Oncogene* **9**, 3717-3729
26. Mackenzie, I. R., and Rademakers, R. (2008) *Curr Opin Neurol* **21**, 693-700
27. Guo, W., Chen, Y., Zhou, X., Kar, A., Ray, P., Chen, X., Rao, E. J., Yang, M., Ye, H., Zhu, L., Liu, J., Xu, M., Yang, Y., Wang, C., Zhang, D., Bigio, E. H., Mesulam, M., Shen, Y., Xu, Q., Fushimi, K., and Wu, J. Y. (2011) *Nat Struct Mol Biol* **18**, 822-830
28. Kabashi, E., Lin, L., Tradewell, M. L., Dion, P. A., Bercier, V., Bourgouin, P., Rochefort, D., Bel Hadj, S., Durham, H. D., Vande Velde, C., Rouleau, G. A., and Drapeau, P. (2010) *Hum Mol Genet* **19**, 671-683
29. Winton, M. J., Van Deerlin, V. M., Kwong, L. K., Yuan, W., Wood, E. M., Yu, C. E., Schellenberg, G. D., Rademakers, R., Caselli, R., Karydas, A., Trojanowski, J. Q., Miller, B. L., and Lee, V. M. (2008) *FEBS Lett* **582**, 2252-2256
30. Barmada, S. J., Skibinski, G., Korb, E., Rao, E. J., Wu, J. Y., and Finkbeiner, S. (2010) *J Neurosci* **30**, 639-649

31. Liu-Yesucevitz, L., Bilgutay, A., Zhang, Y. J., Vanderwyde, T., Citro, A., Mehta, T., Zaarur, N., McKee, A., Bowser, R., Sherman, M., Petrucelli, L., and Wolozin, B. (2010) *PLoS One* **5**, e13250
32. Ling, S. C., Albuquerque, C. P., Han, J. S., Lagier-Tourenne, C., Tokunaga, S., Zhou, H., and Cleveland, D. W. (2010) *Proc Natl Acad Sci U S A* **107**, 13318-13323
33. Dormann, D., Rodde, R., Edbauer, D., Bentmann, E., Fischer, I., Hruscha, A., Than, M. E., Mackenzie, I. R., Capell, A., Schmid, B., Neumann, M., and Haass, C. (2010) *EMBO J* **29**, 2841-2857
34. Gal, J., Zhang, J., Kwinter, D. M., Zhai, J., Jia, H., Jia, J., and Zhu, H. (2011) *Neurobiol Aging* **32**, 2323
35. Kino, Y., Washizu, C., Aquilanti, E., Okuno, M., Kurosawa, M., Yamada, M., Doi, H., and Nukina, N. (2010) *Nucleic Acids Res* **39**, 2781-2798
36. Ito, D., Seki, M., Tsunoda, Y., Uchiyama, H., and Suzuki, N. (2011) *Ann Neurol* **69**, 152-162
37. Chio, A., Restagno, G., Brunetti, M., Ossola, I., Calvo, A., Mora, G., Sabatelli, M., Monsurro, M. R., Battistini, S., Mandrioli, J., Salvi, F., Spataro, R., Schymick, J., Traynor, B. J., and La Bella, V. (2009) *Neurobiol Aging* **30**, 1272-1275
38. Huang, E. J., Zhang, J., Geser, F., Trojanowski, J. Q., Strober, J. B., Dickson, D. W., Brown, R. H., Jr., Shapiro, B. E., and Lomen-Hoerth, C. (2010) *Brain Pathol* **20**, 1069-1076
39. Baumer, D., Hilton, D., Paine, S. M., Turner, M. R., Lowe, J., Talbot, K., and Ansorge, O. (2010) *Neurology* **75**, 611-618
40. Dormann, D., and Haass, C. (2011) *Trends Neurosci* **34**, 339-348
41. Bosco, D. A., Lemay, N., Ko, H. K., Zhou, H., Burke, C., Kwiatkowski, T. J., Jr., Sapp, P., McKenna-Yasek, D., Brown, R. H., Jr., and Hayward, L. J. (2010) *Hum Mol Genet* **19**, 4160-4175
42. Fujita, K., Ito, H., Nakano, S., Kinoshita, Y., Wate, R., and Kusaka, H. (2008) *Acta Neuropathologica* **116**, 439-445
43. Anderson, P., and Kedersha, N. (2006) *J Cell Biol* **172**, 803-808
44. Kedersha, N., and Anderson, P. (2007) *Methods Enzymol* **431**, 61-81
45. Kayali, F., Montie, H. L., Rafols, J. A., and DeGracia, D. J. (2005) *Neuroscience* **134**, 1223-1245
46. DeGracia, D. J., Rudolph, J., Roberts, G. G., Rafols, J. A., and Wang, J. (2007) *Neuroscience* **146**, 562-572
47. Moeller, B. J., Cao, Y., Li, C. Y., and Dewhirst, M. W. (2004) *Cancer Cell* **5**, 429-441
48. Gilks, N., Kedersha, N., Ayodele, M., Shen, L., Stoecklin, G., Dember, L. M., and Anderson, P. (2004) *Mol Biol Cell* **15**, 5383-5398
49. Furukawa, Y., Kaneko, K., Matsumoto, G., Kurosawa, M., and Nukina, N. (2009) *J Neurosci* **29**, 5153-5162
50. Colombrita, C., Zennaro, E., Fallini, C., Weber, M., Sommacal, A., Buratti, E., Silani, V., and Ratti, A. (2009) *Journal of Neurochemistry* **111**, 1051-1061
51. Dewey, C. M., Cenik, B., Sephton, C. F., Dries, D. R., Mayer, P., 3rd, Good, S. K., Johnson, B. A., Herz, J., and Yu, G. (2011) *Mol Cell Biol* **31**, 1098-1108
52. Moisse, K., Volkening, K., Leystra-Lantz, C., Welch, I., Hill, T., and Strong, M. J. (2009) *Brain Res* **1249**, 202-211
53. Meyerowitz, J., Parker, S. J., Vella, L. J., Ng, D., Price, K. A., Liddell, J. R., Caragounis, A., Li, Q. X., Masters, C. L., Nonaka, T., Hasegawa, M., Bogoyevitch, M. A., Kanninen, K. M., Crouch, P. J., and White, A. R. (2011) *Molecular Neurodegeneration* **6**, 57
54. McDonald, K. K., Aulas, A., Destroismaisons, L., Pickles, S., Beleac, E., Camu, W., Rouleau, G. A., and Vande Velde, C. (2011) *Hum Mol Genet* **20**, 1400-10
55. Dewey, C. M., Cenik, B., Sephton, C. F., Johnson, B. A., Herz, J., and Yu, G. (2012) *Brain Res*
56. Freibaum, B. D., Chitta, R. K., High, A. A., and Taylor, J. P. (2010) *J Proteome Res* **9**, 1104-1120
57. Volkening, K., Leystra-Lantz, C., Yang, W., Jaffee, H., and Strong, M. J. (2009) *Brain Res* **1305**, 168-182
58. Kaech, S., and Banker, G. (2006) *Nature Protocols* **1**, 2406-2415

59. Igaz, L. M., Kwong, L. K., Xu, Y., Truax, A. C., Uryu, K., Neumann, M., Clark, C. M., Elman, L. B., Miller, B. L., Grossman, M., McCluskey, L. F., Trojanowski, J. Q., and Lee, V. M. (2008) *The American Journal of Pathology* **173**, 182-194
60. Neumann, M., Kwong, L. K., Lee, E. B., Kremmer, E., Flatley, A., Xu, Y., Forman, M. S., Troost, D., Kretzschmar, H. A., Trojanowski, J. Q., and Lee, V. M. (2009) *Acta Neuropathologica* **117**, 137-49
61. Dormann, D., Capell, A., Carlson, A. M., Shankaran, S. S., Rodde, R., Neumann, M., Kremmer, E., Matsuwaki, T., Yamanouchi, K., Nishihara, M., and Haass, C. (2009) *Journal of Neurochemistry* **110**, 1082-94
62. Winton, M. J., Igaz, L. M., Wong, M. M., Kwong, L. K., Trojanowski, J. Q., and Lee, V. M. (2008) *The Journal of Biological Chemistry* **283**, 13302-13309
63. Mackenzie, I. R., Neumann, M., Baborie, A., Sampathu, D. M., Du Plessis, D., Jaros, E., Perry, R. H., Trojanowski, J. Q., Mann, D. M., and Lee, V. M. (2011) *Acta Neuropathologica* **122**, 111-113
64. Kosugi, S., Hasebe, M., Entani, T., Takayama, S., Tomita, M., and Yanagawa, H. (2008) *Chem Biol* **15**, 940-949
65. Sato, T., Takeuchi, S., Saito, A., Ding, W., Bamba, H., Matsuura, H., Hisa, Y., Tooyama, I., and Urushitani, M. (2009) *Neuroscience* **164**, 1565-1578
66. Nishimura, A. L., Zupunski, V., Troakes, C., Kathe, C., Fratta, P., Howell, M., Gallo, J. M., Hortobagyi, T., Shaw, C. E., and Rogelj, B. (2010) *Brain* **133**, 1763-1771
67. Polymenidou, M., Lagier-Tourenne, C., Hutt, K. R., Huelga, S. C., Moran, J., Liang, T. Y., Ling, S. C., Sun, E., Wancewicz, E., Mazur, C., Kordasiewicz, H., Sedaghat, Y., Donohue, J. P., Shiue, L., Bennett, C. F., Yeo, G. W., and Cleveland, D. W. (2011) *Nat Neurosci* **14**, 459-468
68. Burd, C. G., and Dreyfuss, G. (1994) *Science* **265**, 615-621
69. Hoell, J. I., Larsson, E., Runge, S., Nusbaum, J. D., Duggimpudi, S., Farazi, T. A., Hafner, M., Borkhardt, A., Sander, C., and Tuschl, T. (2011) *Nat Struct Mol Biol* **18**, 1428-31
70. Kim, S. H., Shanware, N. P., Bowler, M. J., and Tibbetts, R. S. (2010) *The Journal of biological Chemistry* **285**, 34097-34105
71. Barber, S. C., and Shaw, P. J. (2010) *Free Radical Biology & Medicine* **48**, 629-641
72. Saxena, S., and Caroni, P. (2011) *Neuron* **71**, 35-48
73. Quaegebeur, A., Lange, C., and Carmeliet, P. (2011) *Neuron* **71**, 406-424
74. Polymenidou, M., and Cleveland, D. W. (2011) *Cell* **147**, 498-508
75. Zhang, Y. J., Xu, Y. F., Dickey, C. A., Buratti, E., Baralle, F., Bailey, R., Pickering-Brown, S., Dickson, D., and Petrucelli, L. (2007) *J Neurosci* **27**, 10530-10534

FOOTNOTES

This work was supported by the Sonderforschungsbereich Molecular Mechanisms of Neurodegeneration (SFB 596), the Competence Network for Neurodegenerative Diseases (KNDD) of the Bundesministerium für Bildung und Forschung (BMBF), and an EMBO post-doctoral fellowship (to D.D.). C.H. is supported by a 'Forschungsprofessur' of the Ludwig-Maximilians University. D.D. is supported by the Robert Bosch Foundation. We thank Claudia Abou-Ajram, Andrea Seibel and Stephanie Kunath for technical assistance. We are grateful to the Hans and Ilse Breuer Foundation for the Confocal Microscope.

FIGURE LEGENDS

FIGURE 1. **Cytosolic FUS is recruited to SG upon treatment with various stressors.**
(A) Schematic diagram of FUS wild-type (WT) and P525L mutant used for transient transfection in HeLa cells. HA = HA epitope tag; Q = glutamine-rich domain; G = glycine-rich domain; R = RNA recognition motif (RRM) domain; Z = arginine-glycine-glycine (RGG) zinc finger domain; PY = proline tyrosine nuclear localization signal (PY-NLS).

(B) HeLa cells were transiently transfected with N-terminally HA-tagged FUS-WT or FUS-P525L. 24 hours after transfection, cells were subjected to heat shock (44°C for 1 hour), sodium arsenite (0.5 mM for 30 min) or clotrimazole (20 µM for 30 min) or were left untreated (control). Cells were fixed, stained with an HA-specific antibody (green), a TIA-1-specific antibody (red) and a nuclear counterstain (blue) and analyzed by confocal microscopy. Panels to the right show a higher magnification of the boxed region. While FUS-WT remained nuclear, FUS-P525L was sequestered into SG under all stress conditions examined. Scale bars: 20 µm.
(C) Primary rat hippocampal neurons were transiently transfected with HA-FUS-WT or P525L on DIV 7. 48 hours after transfection, neurons were subjected to heat shock (44°C) for 1 hour or left untreated (37°C). Neurons were fixed and stained with an HA-specific antibody (green), a TIA-1-specific antibody (red) and the neuronal marker antibody Tuj1 (white) to visualize neuronal morphology. FUS-P525L showed cytoplasmic mislocalization and was recruited to TIA-1-positive SG upon heat stress. Insets in the upper right corner show a higher magnification of the boxed region. Scale bars: 20 µm.

FIGURE 2. **The C-terminal RGG-zinc finger domain of FUS is the most important domain for SG recruitment.**
(A) Schematic diagram of different FUS constructs analyzed for SG recruitment. The P525L mutation was introduced into the PY-NLS to obtain proteins mislocalized in the cytosol.
(B) Immunocytochemistry of HeLa cells expressing the different FUS constructs shown in (A). Prior to fixation, cells were subjected to heat shock (44°C for 1 hour) or left untreated (37°C). Cells were stained with an HA-specific antibody (green), a TIA-1-specific antibody (red) and a nuclear counterstain (blue) and analyzed by confocal microscopy. Panels to the right show a higher magnification of the boxed region. The Z domain is most important for SG recruitment, whereas the Q domain is dispensable. The G and R domains also contribute to SG recruitment, but to a lesser extent than Z. Scale bars = 20 µm.
(C) The percentage of FUS localized in TIA-1-positive SG was quantified using ImageJ. 10-20 cells were analyzed in a blinded manner, means across all cells were calculated and standard deviations are indicated by error bars. Note that the percentage of FUS-P525L in SG seems surprisingly low when looking at the corresponding confocal images in (B). However, SG are very small compared to the remaining cellular volume and therefore FUS-P525L diffusely distributed in the cytosol and nucleus amounts to a significant percentage of the total protein (more than 80%).

FIGURE 3. **The RGG-zinc finger domain of FUS binds to UG-rich RNA.**
(A) FUS-WT was *in vitro* translated in the presence of [^{35}S]methionine (left lane, input) and was analyzed for binding to different RNA oligonucleotides immobilized on streptavidin beads (right lanes, UG_{12} = UGUGUGUGUGUGUGUGUGUGUG; GGUG = UUGUAUUUUGAGCUAGUUUGGUGAU; CCUC = UUGUAUUUUGAGCUAGUUUCCUCAU). FUS was pulled down most efficiently by UG_{12} and to a lesser extent by GGUG RNA.
(B) The indicated FUS constructs were *in vitro* translated in the presence of [^{35}S]methionine (upper panel, input). Biotinylated UG_{12} RNA immobilized on streptavidin beads was used to pull down radioactively labeled proteins (lower panel, pulldown). CCUC RNA was used as a negative control. FUS-WT and P525L and all proteins comprising the Z_{P525L} domain were specifically pulled down by UG_{12} RNA, while the other proteins did not show detectable RNA binding. Open arrowheads indicate degradation products.

FIGURE 4. **Cytosolic mislocalization is a prerequisite for SG recruitment of TDP-43.**
(A) Schematic diagram of TDP-43 wild-type (WT) and NLS mutant (NLSmut). NLSmut = triple point mutation in the classical nuclear localization signal (K83A/R84A/K85A); RRM = RNA recognition motif domain; G-rich = glycine-rich domain; V5 = V5 epitope tag.
(B) C-terminally V5-tagged TDP-WT or NLSmut were transiently transfected into HeLa cells and 24 hours later were subjected to heat shock (44°C for 1 hour), sodium arsenite (0.5 mM for 30 min) or clotrimazole (20 µM for 30 min) treatment or were left untreated (control). Cells were fixed, stained with a V5 (green) and TIA-1 (red)-specific antibody and a nuclear counterstain (blue) and analyzed by confocal microscopy.

Panels to the right show a higher magnification of the boxed region. While the cytosolic NLS mutant was sequestered into SG, TDP-WT remained nuclear under all stress conditions examined. Scale bars = 20 µm.
(C) Primary rat hippocampal neurons were transiently transfected with V5-tagged TDP-WT or NLSmut. 48 hours post-transfection, neurons were subjected to heat shock (44°C) for 1 hour or left untreated (37°C). Neurons were fixed and stained with a V5-specific antibody (green), a TIA-1-specific antibody (red) and the neuronal marker antibody Tuj1 (white) to visualize neuronal morphology. NLSmut showed partial cytoplasmic mislocalization and was recruited to TIA-1-positive SG upon heat stress. Insets in the upper right corner show a higher magnification of the boxed region. Scale bars: 20 µm.

FIGURE 5. **Endogenous TDP-43 is sequestered into heat shock-induced SG upon inhibition of Importin α/β-dependent nuclear import.**
HeLa cells were transfected with an Importin α/β-specific peptide inhibitor fused to GFP (GFP-Bimax) or GFP as a control (green). 24 hours post-transfection cells were subjected to heat shock (44°C for 1 hour) or kept at control temperature (37°C) prior to fixation. Cells were co-stained for endogenous TDP-43 (red) and TIA-1 (white) and analyzed by confocal microscopy. Expression of GFP-Bimax resulted in cytosolic mislocalization of endogenous TDP-43 and recruitment into SG upon heat shock. Under control conditions (GFP), TDP-43 was predominantly nuclear and did not colocalize with SG after heat shock. Scale bars = 20 µm.

FIGURE 6. **ALS-associated *TARDBP* mutations do not alter the cellular localization of TDP-43.**
(A) Myc-tagged wild-type TDP-WT or TDP-43 carrying the indicated ALS-associated point mutations (A315T, M337V or G348C) were transiently transfected into HeLa cells. 24 hours post-transfection cells were subjected to heat shock (44°C for 1 hour) or kept at control temperature (37°C). Afterwards cells were fixed, stained with a myc (green) and TIA-1 (red)-specific antibody and a nuclei counterstain (blue) and analyzed by confocal microscopy. Both TDP-WT and the ALS-associated point mutants were nuclear under control conditions and remained nuclear upon heat shock. Scale bars = 20 µm.
(B) Expression level of TDP-43 constructs used in (A). Total cell lysates were analyzed by immunoblotting with a myc-specific antibody (upper panel). Tubulin served as a loading control (lower panel). All lanes were from the same exposure of the same blot.
(C) Quantification of nuclear and cytosolic fluorescence intensities of myc staining at 37°C. Error bars indicate standard deviations.

FIGURE 7. **ALS-associated *TARDBP* mutations do not affect SG recruitment of cytosolic TDP-43.**
ALS-associated point mutations (A315T, M337V, G348C) were introduced into the TDP-43 NLS mutant ($NLSmut_{A315T}$, $NLSmut_{M337V}$, $NLSmut_{G348C}$) and effect of mutations on SG recruitment was analyzed.
(A) HeLa cells transiently transfected with the indicated TDP-43 constructs were incubated with clotrimazole for 30 min or left untreated (control). Cells were fixed, stained with a V5 (green) and TIA-1 (red)-specific antibody and a nuclear counterstain (blue) and analyzed by confocal microscopy. ALS-associated point mutations did not affect SG recruitment of cytosolic TDP-43. Scale bars = 20 µm.
(B) Protein levels in total cell lysates were analyzed by immunoblotting with a V5-specific antibody (upper panel), Tubulin served as a loading control (lower panel). Black arrowhead indicates full-length TDP-43, white arrowhead indicates caspase-generated 35 kDa C-terminal fragment (CTF) frequently observed under transient transfection conditions (61,75).
(C) The percentage of TDP-43 localized in TIA-1-positive SG was quantified using ImageJ. 15-20 cells were analyzed in a blinded manner, means across all cells were calculated and standard deviations are indicated by error bars.

FIGURE 8: **TDP-43 inclusions in spinal cord but not hippocampus are frequently co-labeled for the SG marker protein PABP-1.**
TDP-43 immunohistochemistry performed on formalin-fixed, paraffin-embedded tissue sections of spinal cord (upper panels) or hippocampus (lower panels) from FTLD-TDP and ALS-TDP cases. Staining with

N-terminal and C-terminal TDP-43 specific antibodies demonstrated labeling of neuronal cytoplasmic inclusions in motor neurons in the spinal cord with both antibodies (ALS case #1 shown), whereas inclusions in dentate granule neurons in the hippocampus were labeled only with the C-terminal antibody (FTLD-TDP case #1 shown). Double-label immunofluorescence stainings of the same cases showed co-labeling of phospho-TDP-43 positive inclusions (green) with the SG marker protein PABP-1 (red) in the spinal cord, but not in cortical inclusions. Nuclei were stained with DAPI (blue). Scale bars = 10 µm.

FIGURE 9. **25 kDa C-terminal fragment and a C-terminal deletion mutant of TDP-43 are poorly sequestered into SG.**
(A) Schematic diagram of TDP-43 deletion mutants analyzed for SG recruitment. The deletion mutant Δ1-173 was chosen to mimic the 25 kDa C-terminal fragment (CTF) found to be deposited in cortical regions of FTLD-TDP patients (4,59). The C-terminal deletion mutant (NLSmutΔC) lacks the prion-like glycine-rich domain.
(B) The indicated TDP-43 constructs were transiently transfected in HeLa cells. Prior to fixation, cells were treated with clotrimazole (20 µM, 30 min) or left untreated (control). Subsequently, cells were stained with a V5 (green) and TIA-1 (red)-specific antibody and a nuclear counterstain (blue) and analyzed by confocal microscopy. Panels to the right show a higher magnification of the boxed region. In contrast to full length TDP-NLSmut, both deletion mutants remained predominantly diffuse in the cytosol upon heat shock and were poorly recruited to SG. Scale bars = 20 µm.
(C) The percentage of TDP-43 localized in TIA-1-positive SG was quantified using ImageJ. 15-20 cells were analyzed in a blinded manner, means across all cells were calculated and standard deviations are indicated by error bars.
(D) Protein levels in total cell lysates were analyzed by immunoblotting with a V5-specific antibody (upper panel), Tubulin served as a loading control (lower panel). Black arrowheads indicate full-length TDP-NLSmut or the two deletion mutants, white arrowheads indicate degradation products. All lanes were from the same exposure of the same blot.

FIGURE 10. **The C-terminal deletion mutant of TDP-43 still binds to UG_{12} RNA.**
(A) TDP-WT was *in vitro* translated in the presence of [^{35}S]methionine (left lane, input) and was analyzed for binding to different RNA oligonucleotides immobilized on streptavidin beads (right lanes, UG_{12} = UGUGUGUGUGUGUGUGUGUGUG; GGUG = UUGUAUUUUGAGCUAGUUUGGUGAU; CCUC = UUGUAUUUUGAGCUAGUUUCCUCAU). TDP-43 bound to both UG_{12} and GGUG RNA, but not to CCUC RNA.
(B) The indicated TDP-43 constructs were *in vitro* translated in the presence of [^{35}S]methionine (upper panel, input). Biotinylated UG_{12} RNA or CCUC control RNA were immobilized on streptavidin beads and were used to pull down radioactively labeled proteins (lower panel, pulldown). TDP-WT and NLSmut as well as the C-terminal deletion mutant NLSmut-ΔC were specifically pulled down by UG_{12} RNA, whereas the Δ1-173 deletion mutant resembling the 25 kDa CTF did not bind to UG_{12} RNA.

FIGURE 11. **Model of SG recruitment of TDP-43 and FUS.**
Upon cellular stress, translation of mRNAs is arrested and translationally silent preinitiation complexes that contain mRNA, the small ribosomal subunit (40S), early initiation factors (e.g. eIF3, eIF4A, eIF4G) and PABP-1 are packaged into stress granules (SG). We suggest that recruitment of TDP-43 (left) or FUS (right) into SG involves both protein-RNA and protein-protein interactions. TDP-43 and FUS bind to UG-rich mRNA sequences via their main RNA binding domain (RRM1 in TDP-43 and RGG-zinc finger (Z) domain in FUS, respectively) and thus might be recruited into SG via their associated mRNAs. Since additional domains that did not show binding to UG-rich RNA in our RNA binding assay, also contribute to SG recruitment of TDP-43 and FUS, we suggest that additional protein-protein interactions with proteins X and Y are involved in SG recruitment of TDP-43 and FUS.

Fig. 1

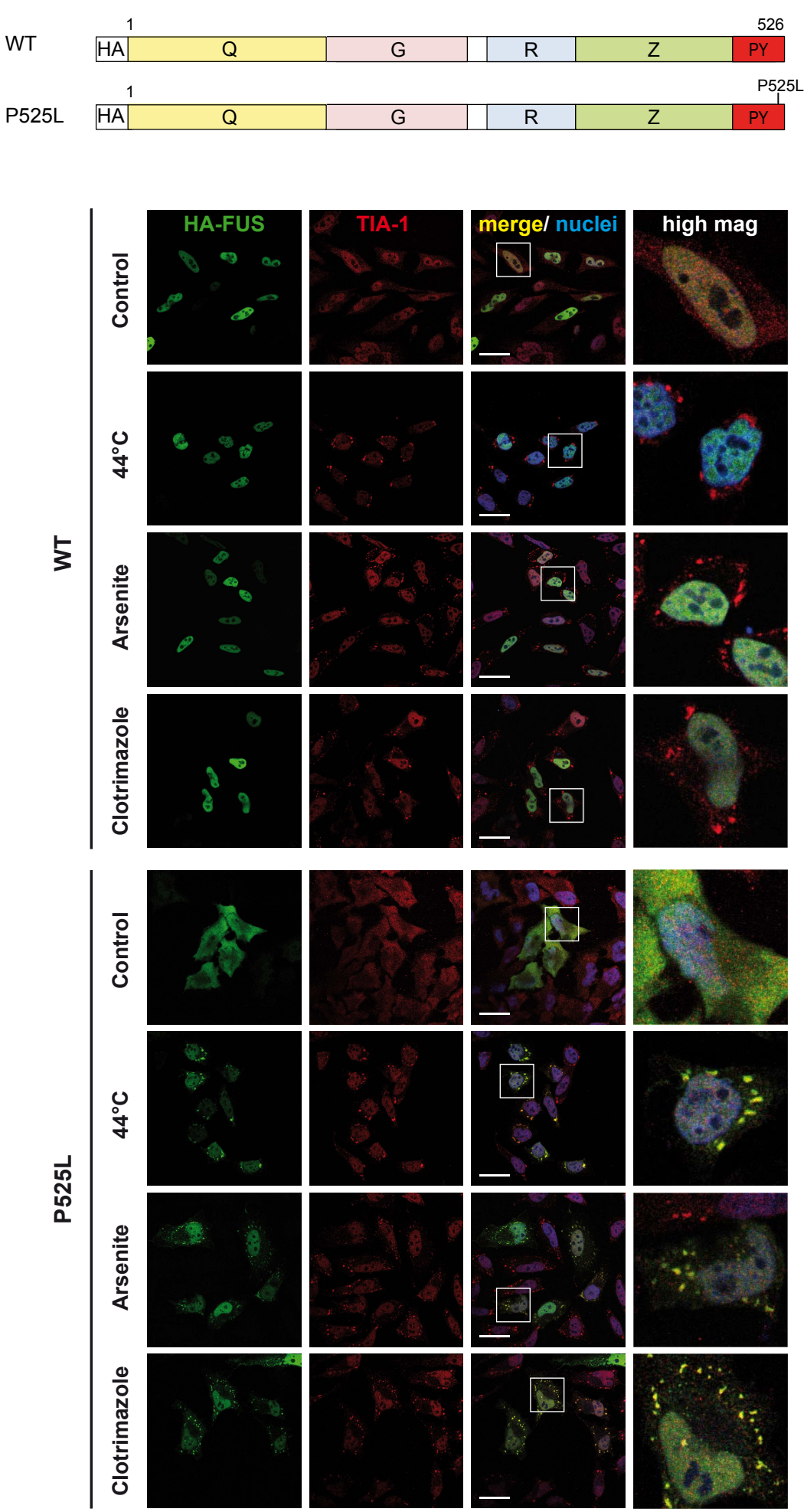

Fig. 1C

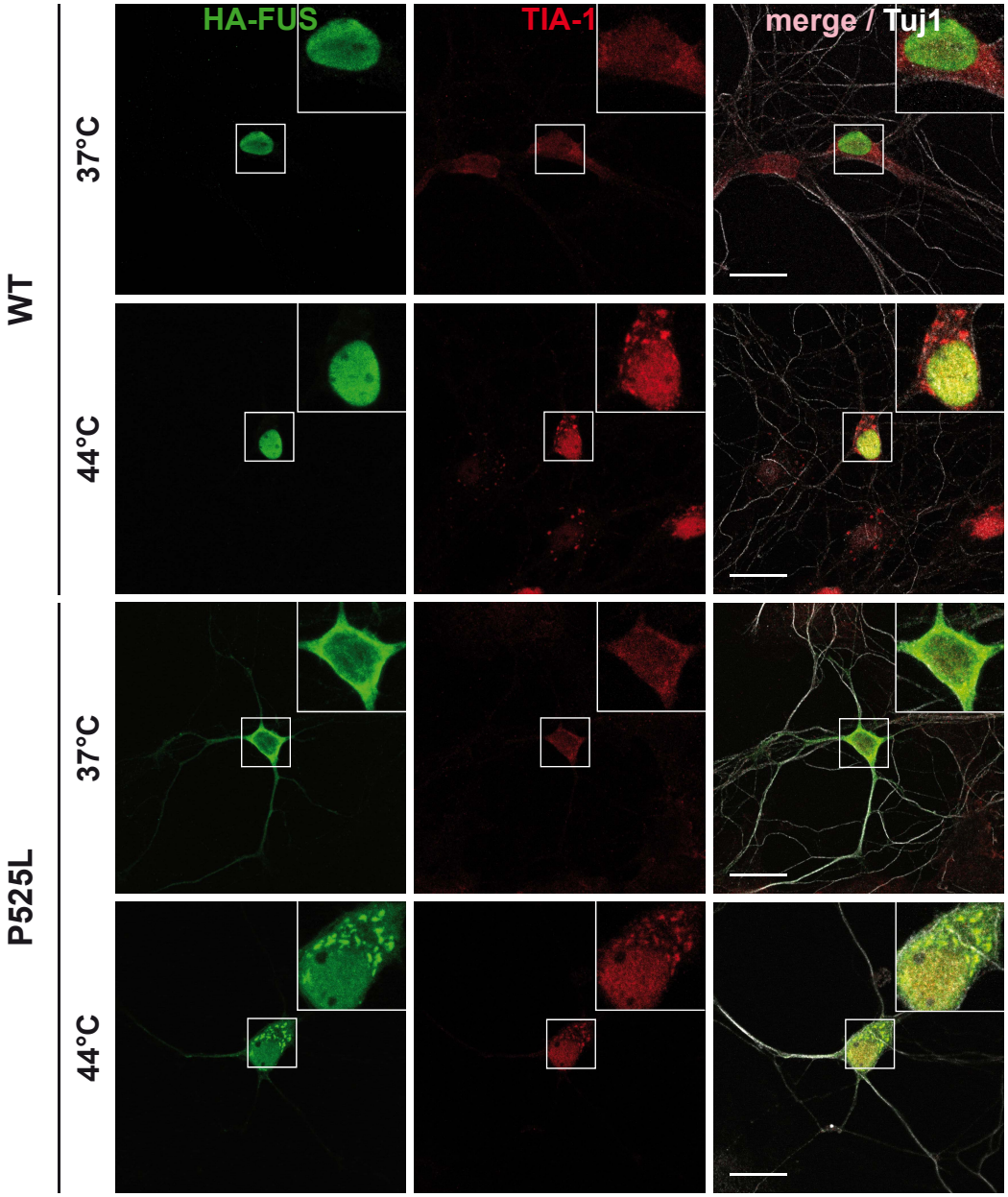

Fig. 2A

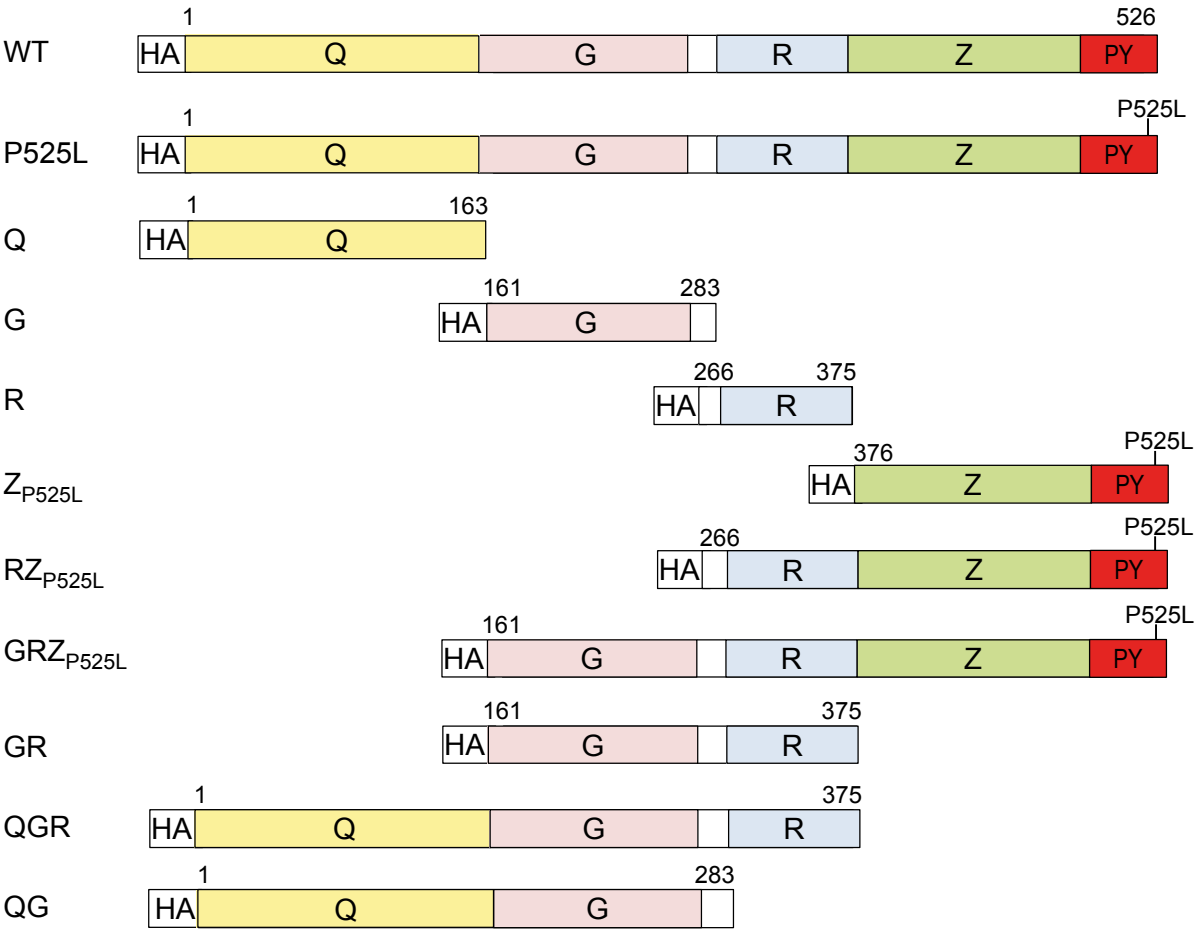

Fig. 2B

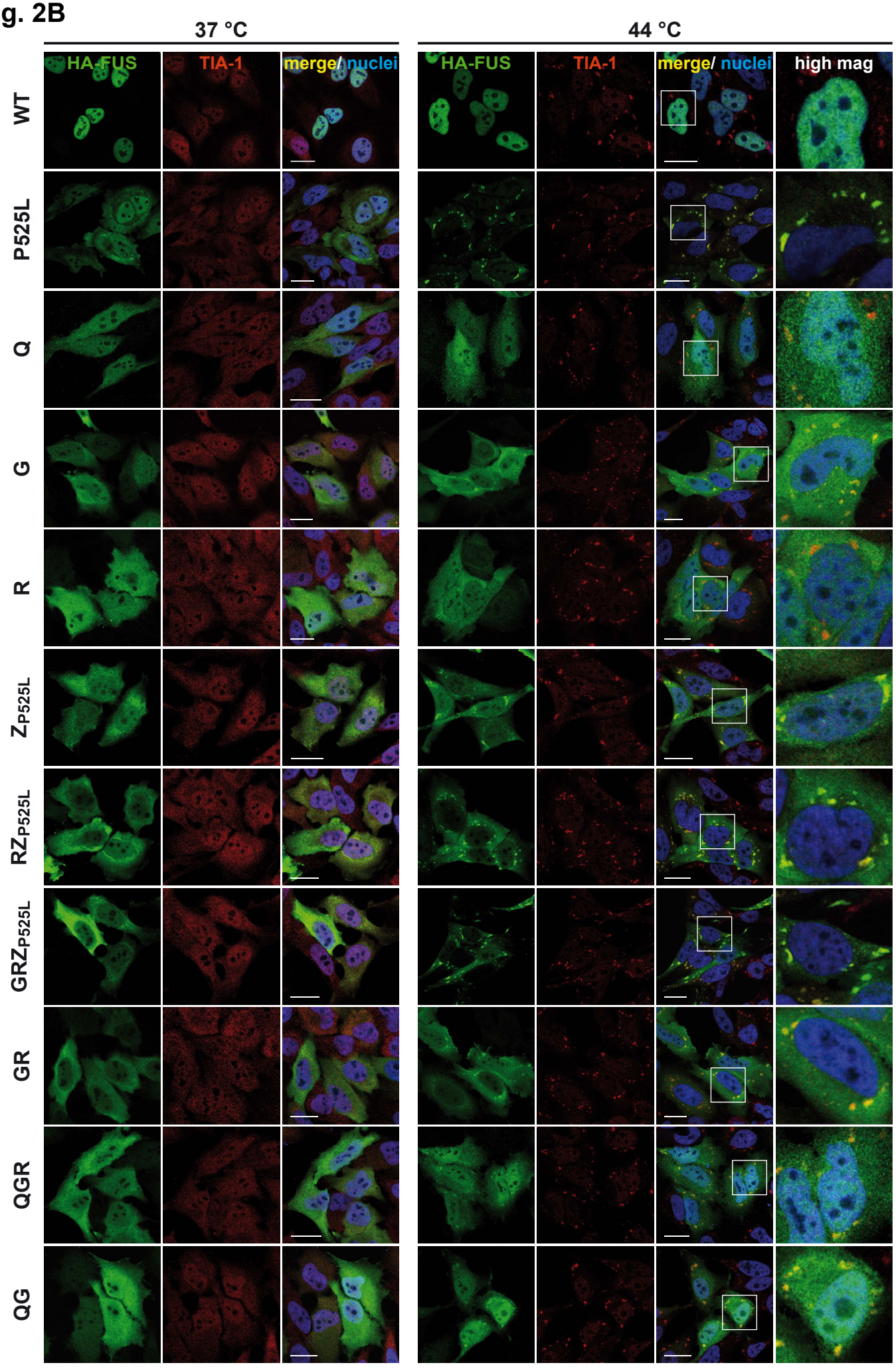

Fig. 2C

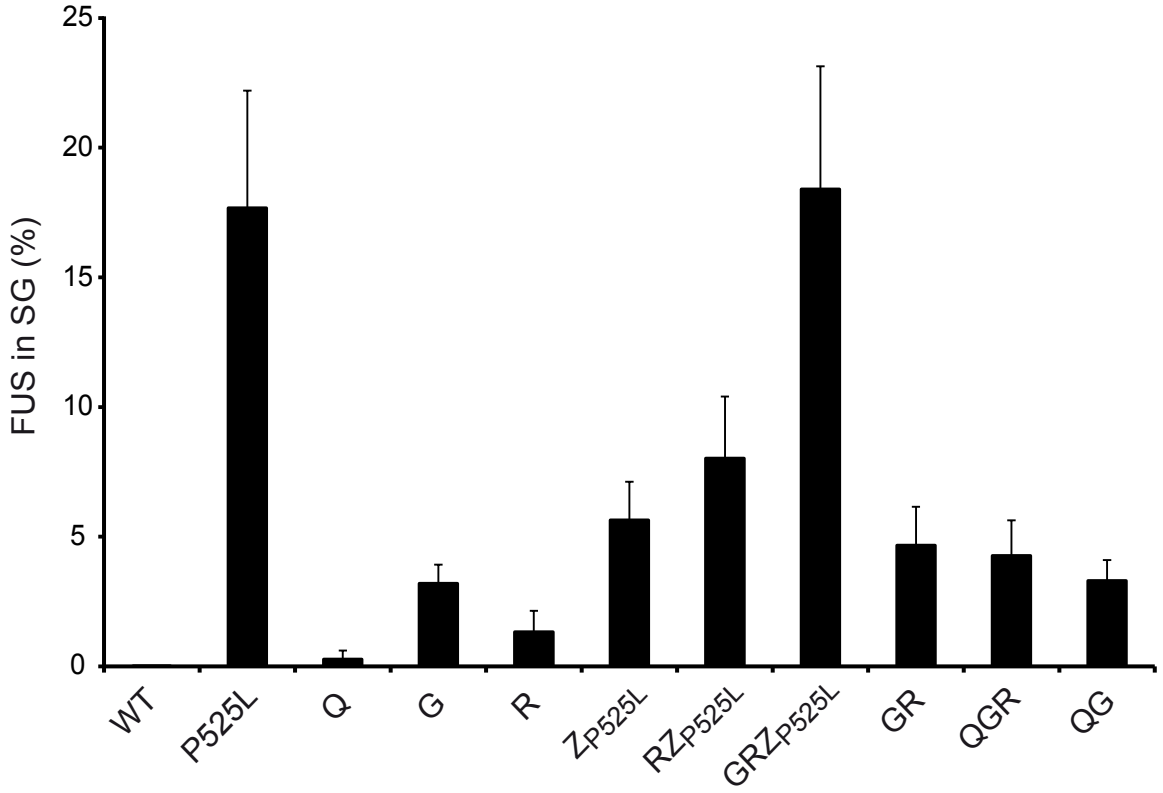

Fig. 3

A

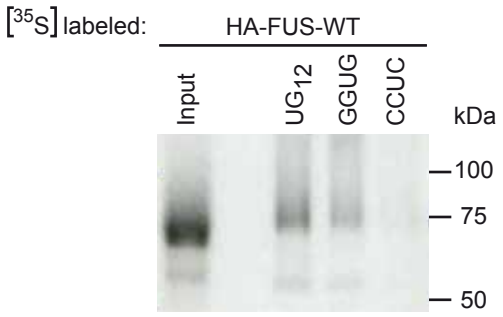

B

Input

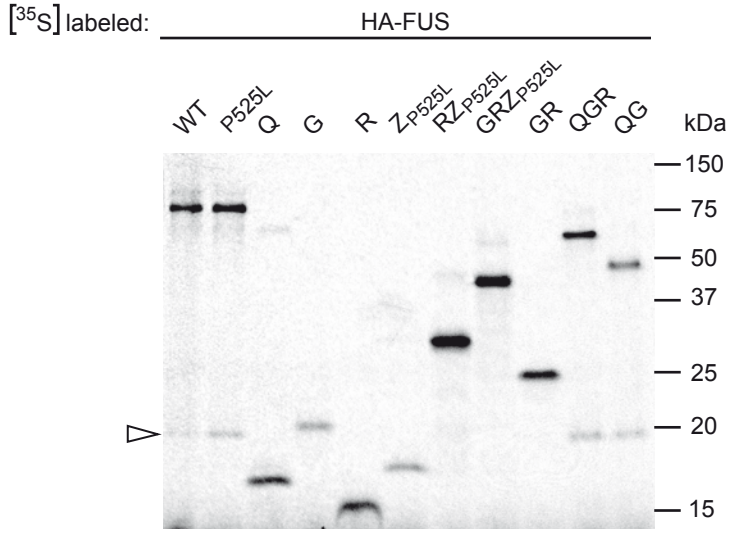

Pulldown

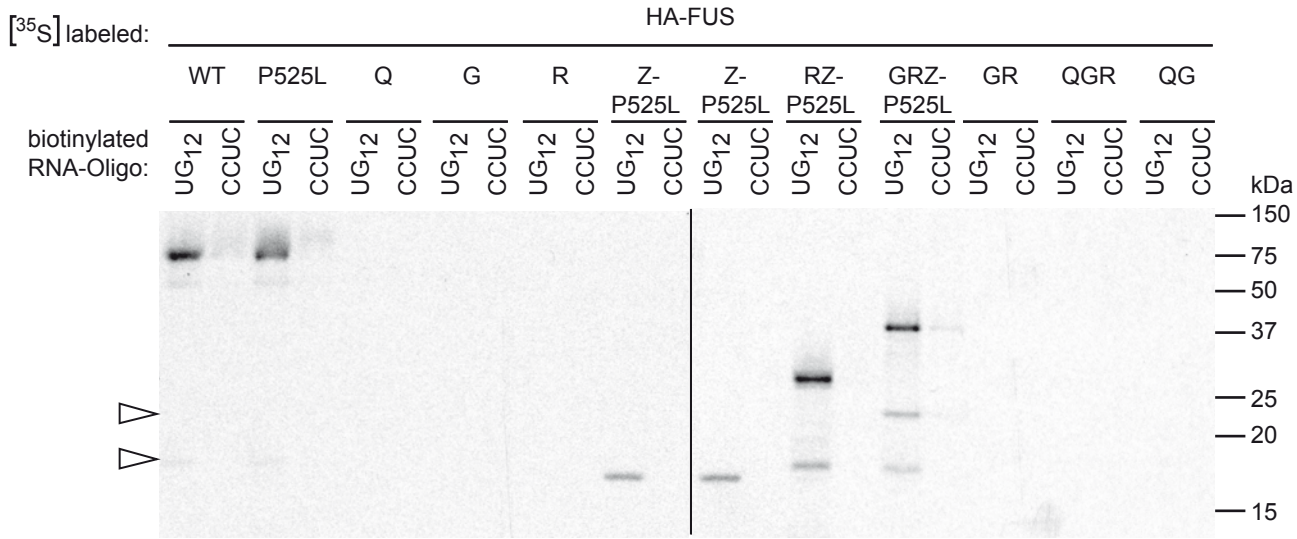

Fig. 4

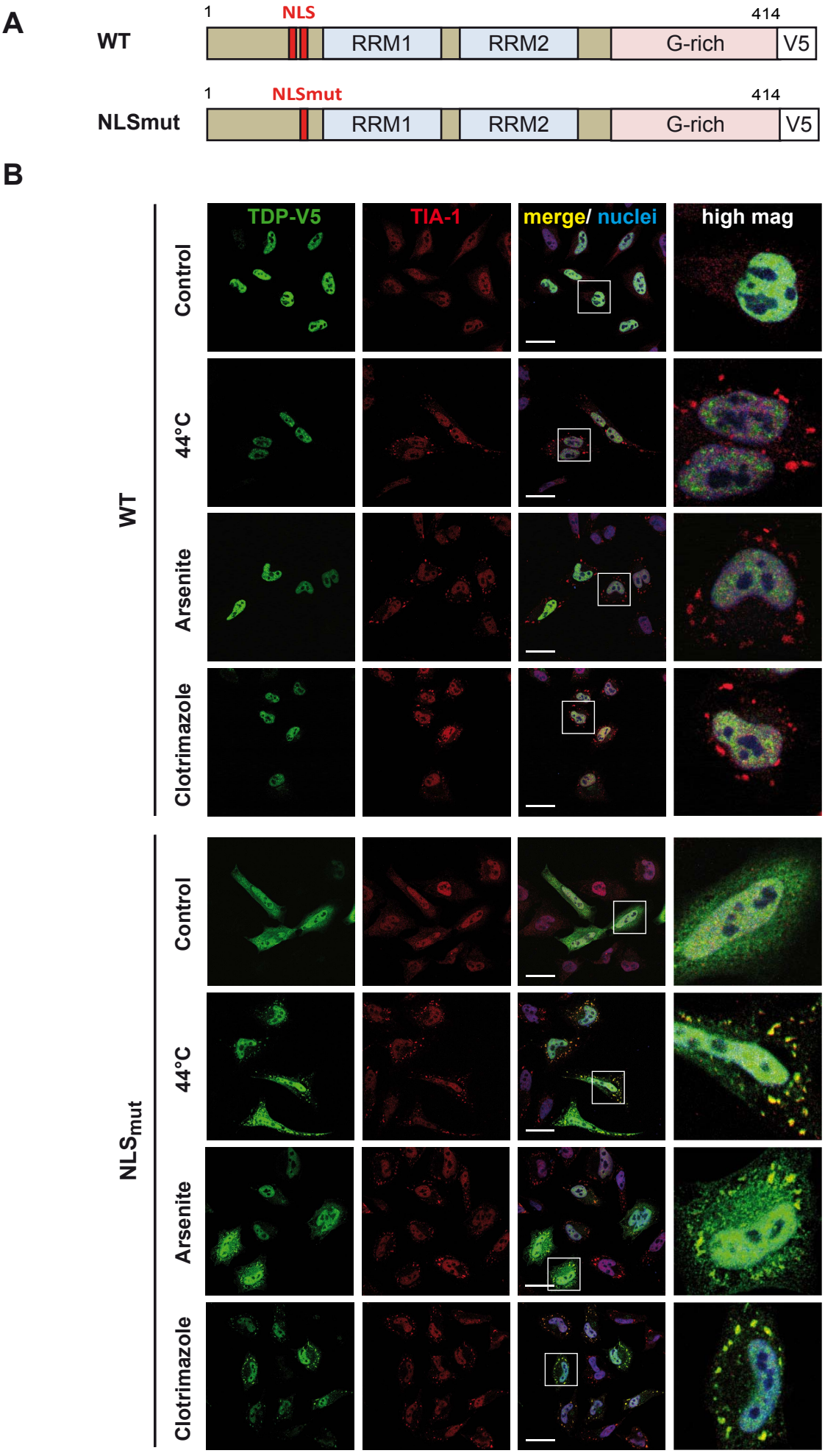

Fig. 4C

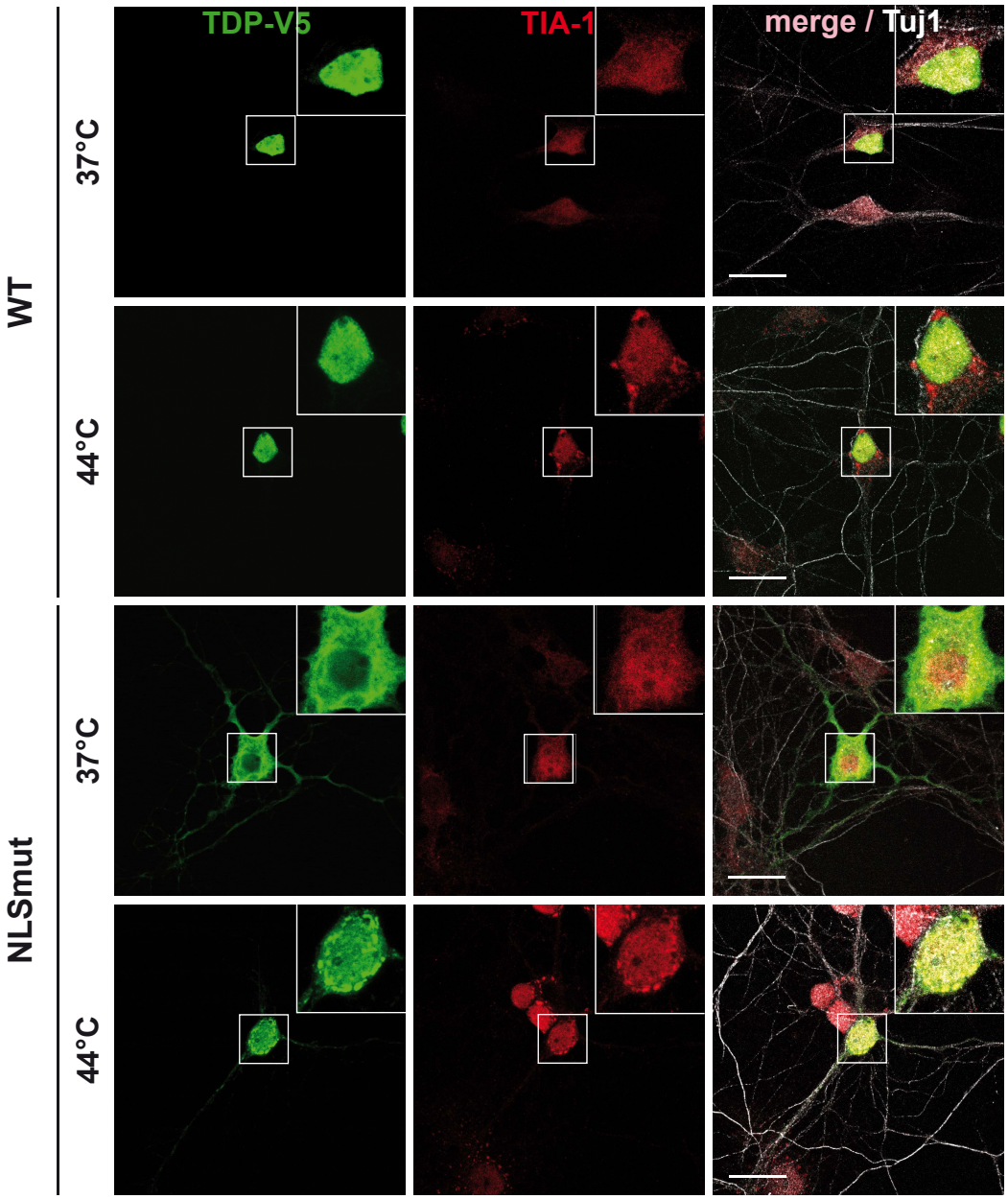

Fig. 5

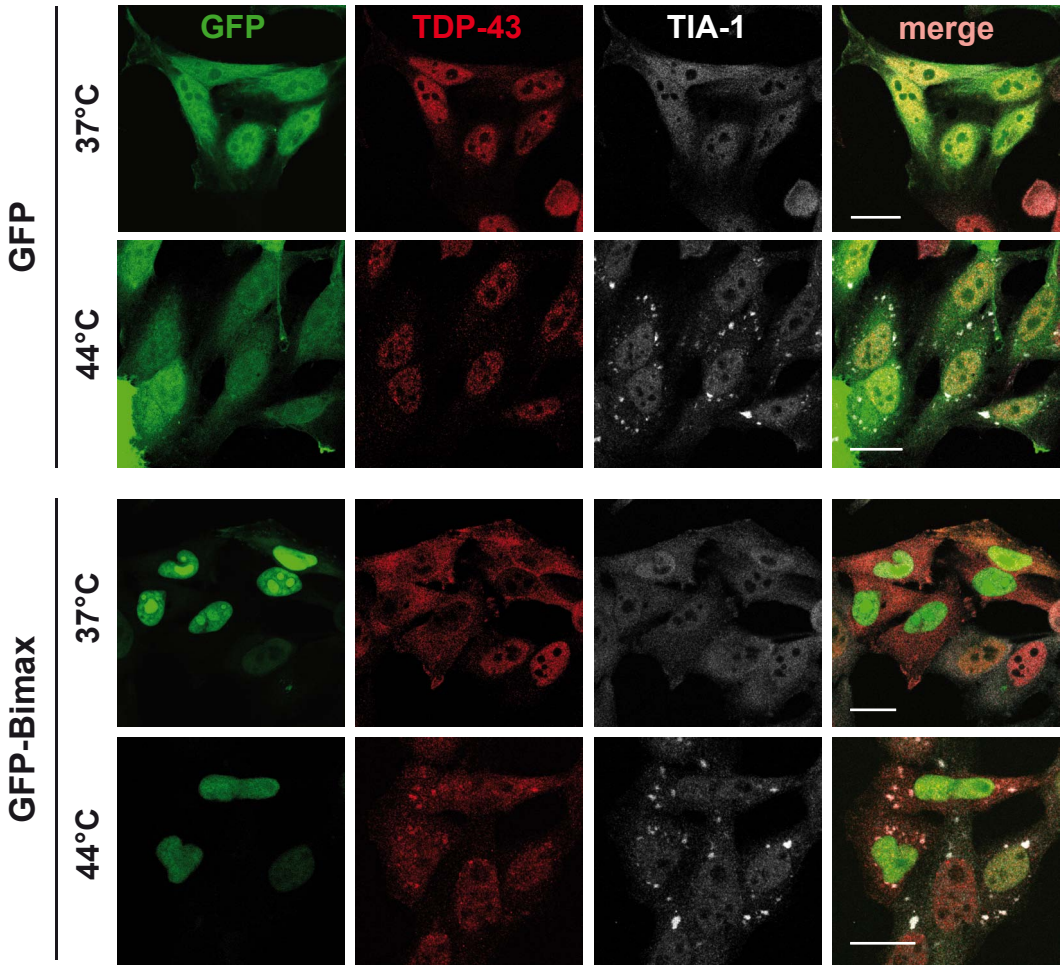

Fig. 6

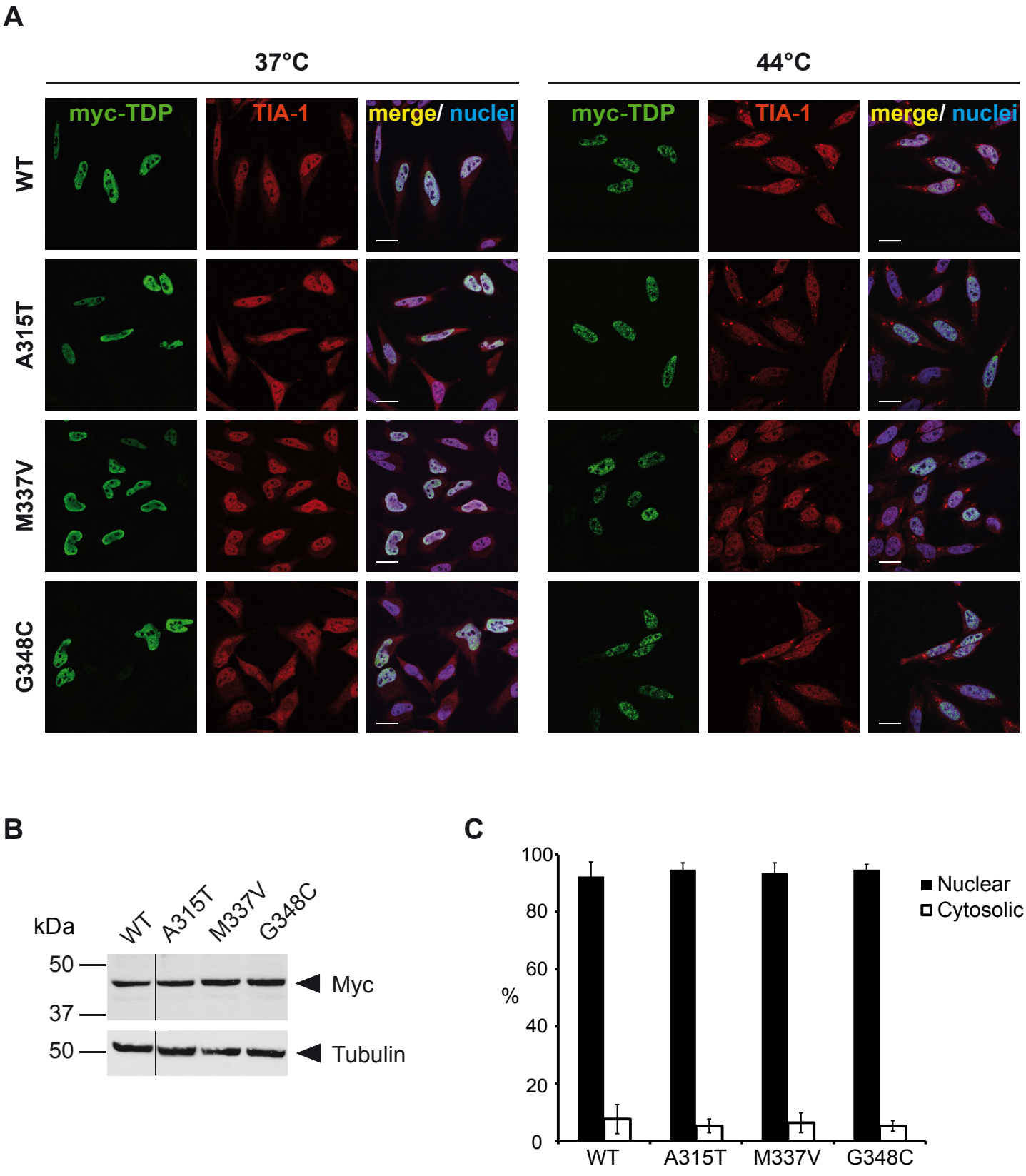

Fig. 7

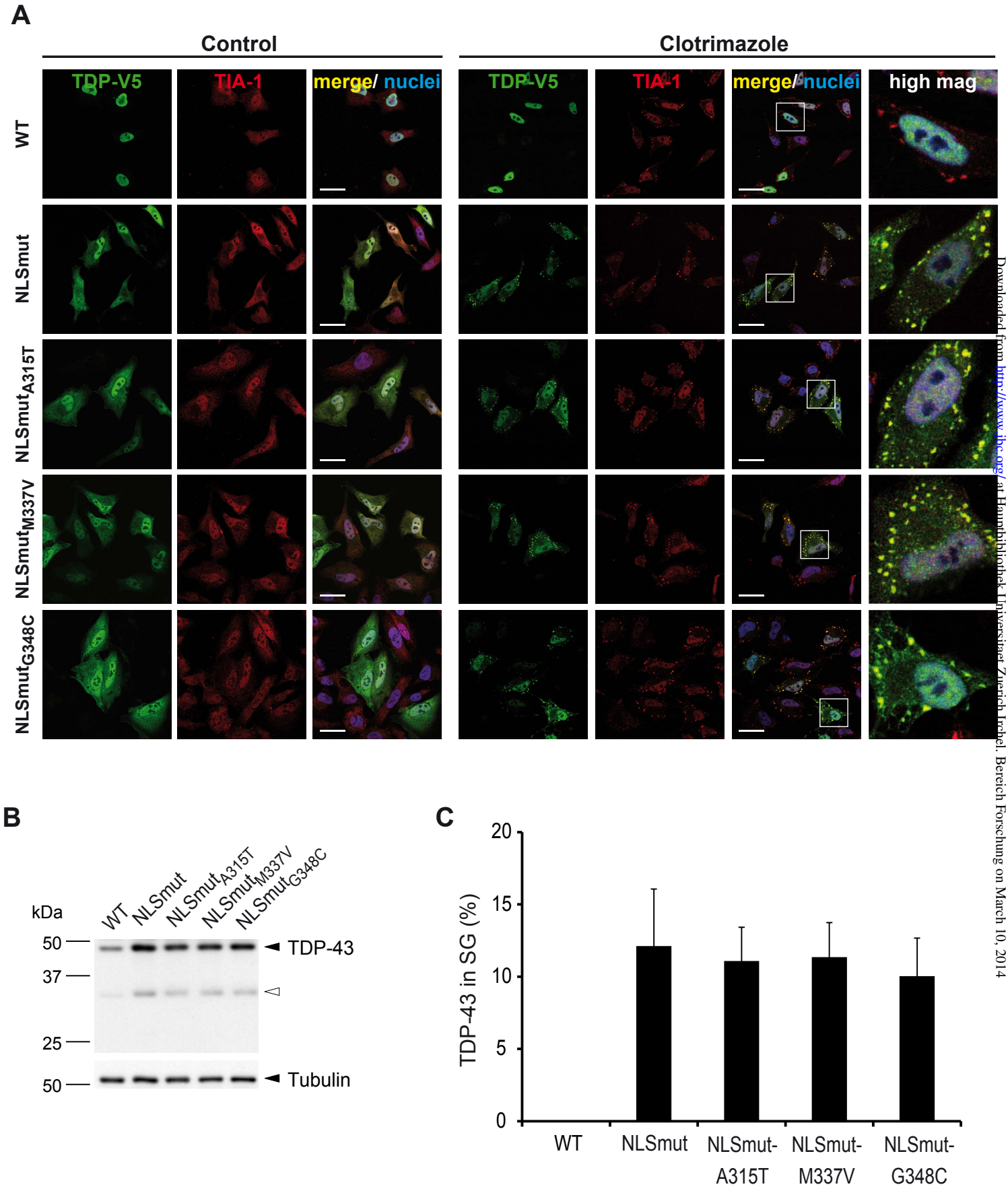

Fig. 8

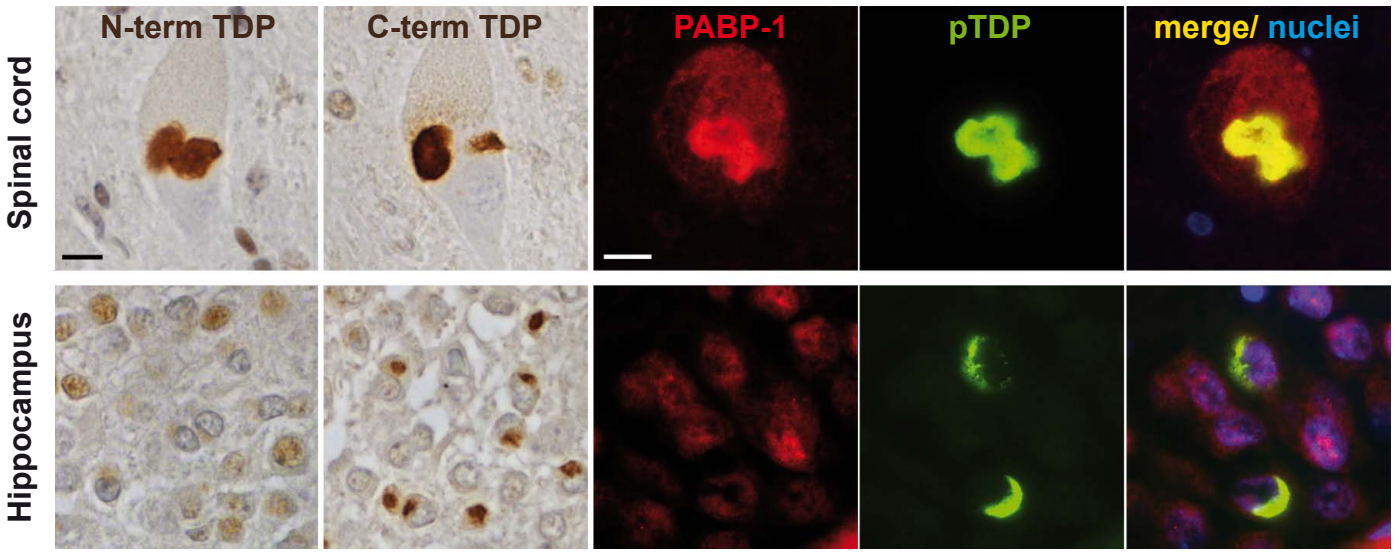

Fig. 9

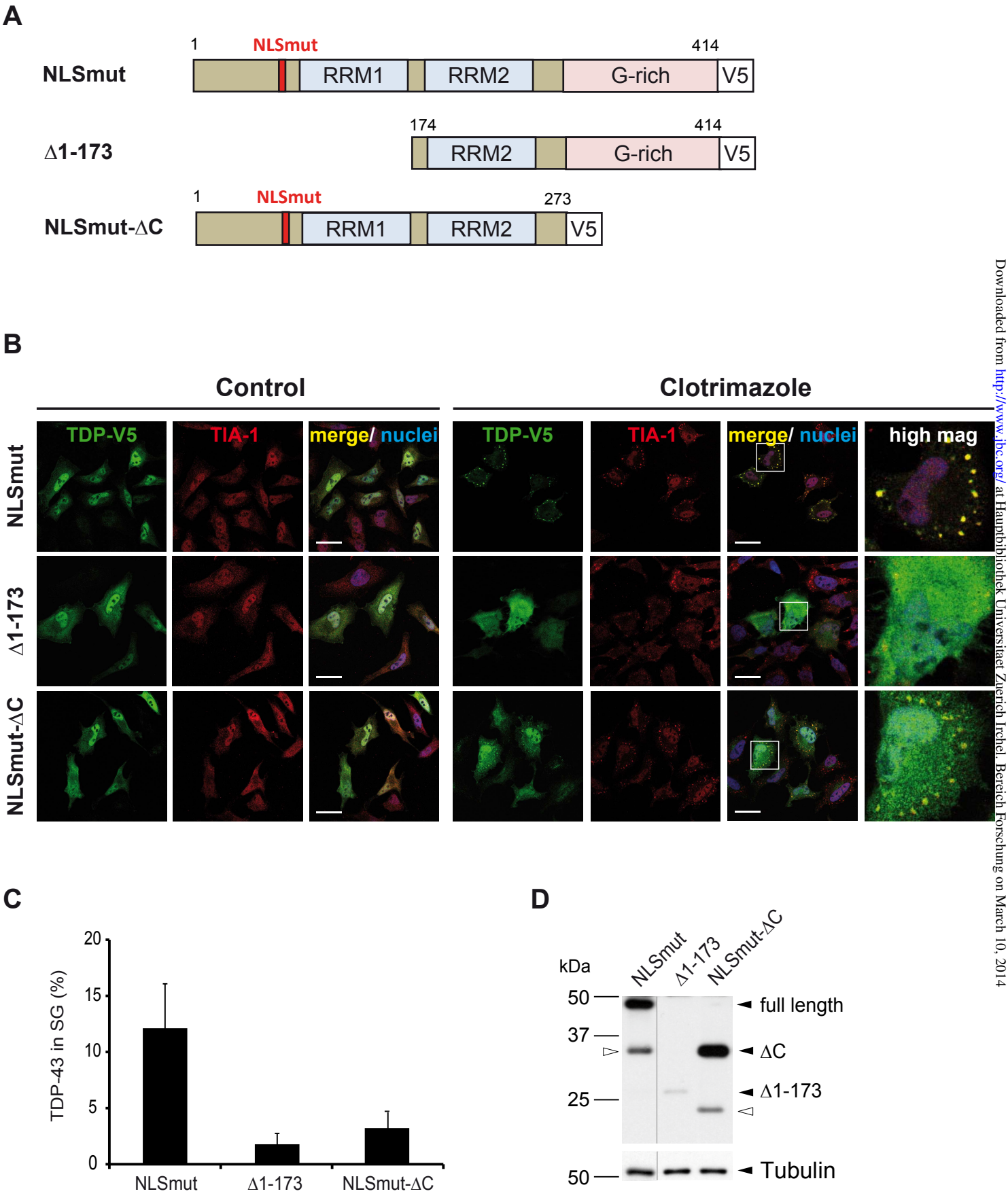

Fig. 10

A

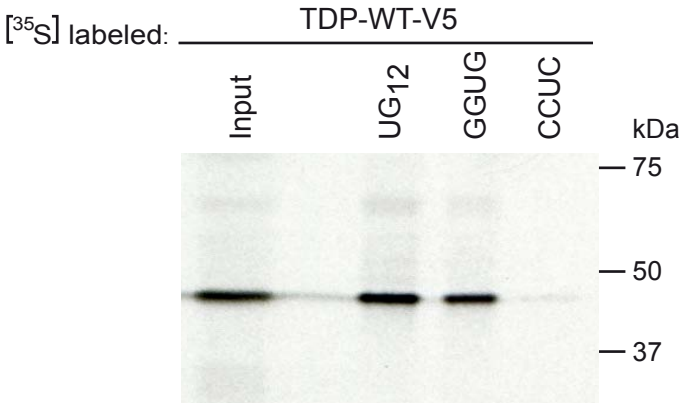

B

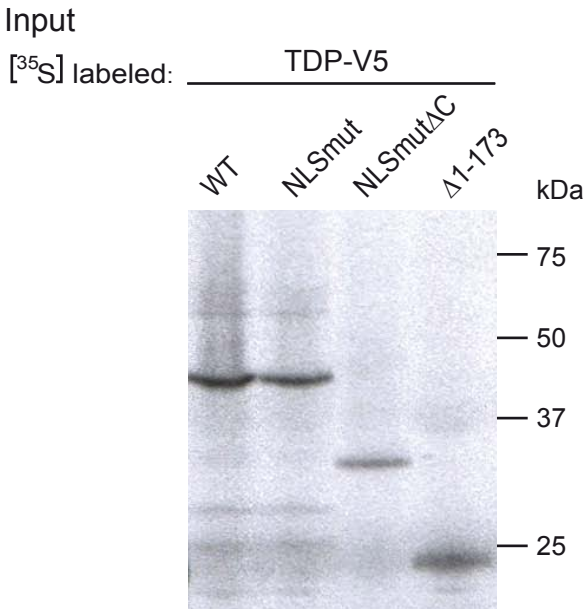

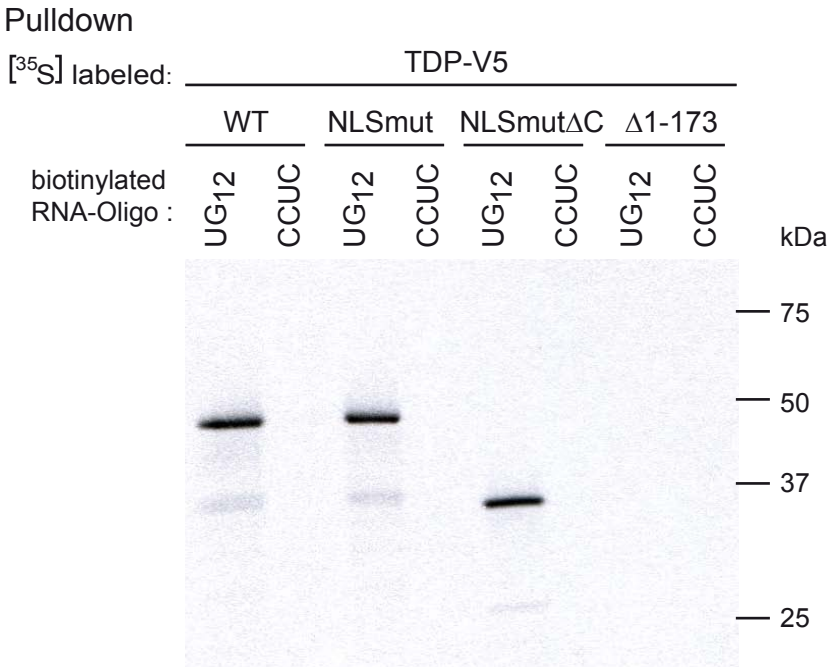

Fig. 11